



VEÐURSTOFA
ÍSLANDS

Report
03037

Halldór Björnsson

The annual cycle of temperature in Iceland

VÍ-ÚR26
Reykjavík
October 2003

Abstract

This report presents the results of an analysis of temperature at weather stations in Iceland. Monthly temperature means for the period 1961 – 1990 were calculated for each station, and the results spatially interpolated.

The spatial interpolation procedure consisted of two steps: de-trending and kriging. In the de-trending step an 8 component linear model was fitted to the temperature data, and the residual from the linear model calculated. In the kriging step, the residuals were spatially interpolated to a map of Iceland using kriging. The results from the linear model were added to the interpolated residual field to produce a map of mean temperature for the month. This method was employed for the 12 calendar months, and also for the annual mean.

Following this, the 12 monthly values at each gridpoint of the map were interpolated to produce a 365 day smooth seasonal cycle. This allowed for a more detailed study of the annual cycle and the calculation of maps of various temperature related indices.

Introduction

When the Icelandic Meteorological Office (IMO) was founded in 1920 it inherited an observation network that had been maintained by the Danish Meteorological Institute since its inception in 1872. The number of stations in this network varied, but was usually between 15 and 20. The IMO network was expanded in the next decades, and during the 30 year period from 1961 to 1990, around 80 manned weather stations were simultaneously in operation. These numbers cover stations where temperature measurements were performed, but do not include stations where only precipitation was measured. Since 1990 the number of manned weather stations has declined, but numerous automatic stations have been installed.

Various climatological parameters have been calculated using data from these stations and primarily reported in *Veðráttan*, which the IMO has published since 1924. Maps of January and July monthly mean temperature for the period 1931 - 1960 were compiled by Eythorsson and Sigtryggsson (1971) and more detailed maps for the same months were presented in the study by Einarsson (1984). The next thirty year period (from 1961 to 1990) is coincidentally the the period with the best data coverage from manned stations in the data IMO archives. Therefore this period is the obvious time-frame to use as a reference period for updating the monthly mean temperature maps.

This report presents maps of monthly mean temperature using 1961 to 1990 as a reference period. Furthermore, a smooth 365 day annual cycle for each gridpoint in the map is calculated, and maps of various indices relating to the annual cycle of temperature are presented.

Data

The data used is described in more detail in Gylfadottir (2003). It comes from the observation network maintained by the IMO (see Figure 1). The manual station network used comprises of 84 stations. The data from these stations is continuous throughout most of the reference period, any gaps were interpolated using nearby station data.

The manual stations tend to be close to the coast with few stations in the highlands. This poses a problem for the interpolation of mean temperature, since the effects of altitude on temperature are poorly represented in the data. This is less of a problem

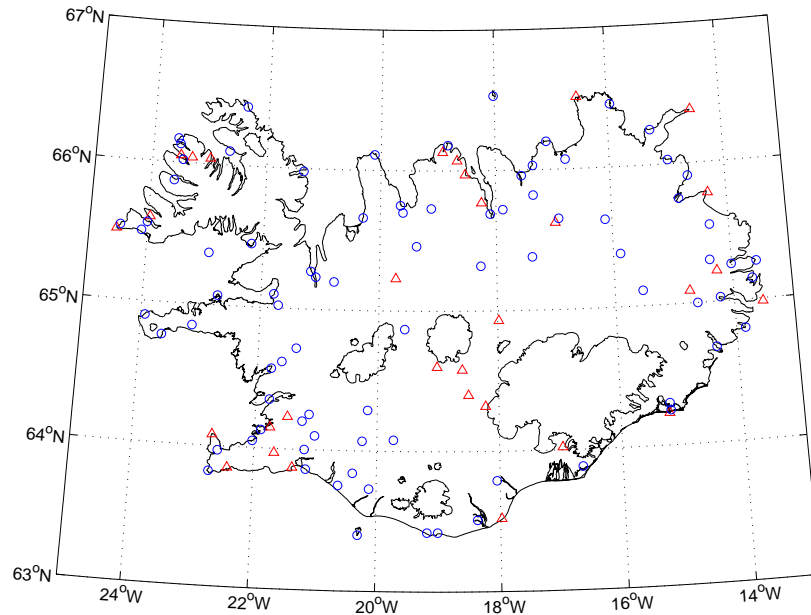


Figure 1: The station network used in this study. The manual stations (blue circles) have been operated throughout the 1961-1990 reference period, whereas the automatic stations (red triangles) have been in operation for less than a decade.

for the interpolation of anomalies (i.e., the monthly departures from the average of the reference period) since most of the altitude effects cancel when anomalies are calculated. In recent years numerous automatic stations have been installed, with several stations in the highlands. In order to better include altitude dependent effects in the database the monthly mean temperature for the reference period (1961 – 1990) at these locations was estimated. For this, the following procedure was applied: First, using the reference period as a baseline, monthly anomalies for the 1990's were calculated using data from the manual station network. Next, for each automatic station, station data and the monthly anomaly at the station location were used to estimate the monthly mean for the reference period at the corresponding station. If the automatic station had been in operation for, say, 5 years this yielded 5 independent estimates of the reference period mean for each calendar month. The average of the five values was then used to represent the monthly mean for the reference period. In this way 31 stations were added to the network. For several stations this method could be tested by comparing the values it produced for an automatic station with those at nearby manual stations. These tests did not reveal bias in the method.

Maps of monthly mean temperature

Method

The construction of the monthly mean temperature maps is performed in two steps. First, the temperature data is “de-trended”. Trend components of the temperature field are found using multiple linear regression on chosen predictands believed to be the

most influential on temperature. A linear model of temperature can then be calculated using gridded maps of the predictands. This linear model does not capture local variability features which will be dominant in the residual field, i.e. the field that describes the difference between the actual temperature and the linear model estimations. This field is found by interpolating the station residuals to the grid using the kriging method.

The predictands used were station longitude (L_x), latitude (L_y), station altitude (ALT), the distance-to-open-ocean (DTO), and the projections of the first four eigenvectors of local topography (EV_1 – EV_4). With these predictands the temperature map for each month was calculated according to the following:

$$T = T_l + R$$

where T_l is the linear model calculated using

$$T_l = a_0 + a_1 \cdot L_x + a_2 \cdot L_y + a_3 \cdot ALT + a_4 \cdot DTO + a_5 \cdot EV_1 + a_6 \cdot EV_2 + a_7 \cdot EV_3 + a_8 \cdot EV_4,$$

and R is the residual field, i.e., the map obtained through applying kriging on the residuals. The a_i parameters in the expression for T_l are found through linear regression on the station data. Below each predictand will be discussed briefly.

The grid used is a latitude-longitude grid with a resolution of half a minute. This means that the average gridcell size is $0.36km^2$. The standard (L_2) norm on a latitude-longitude grid does not conserve true distances, since the distance between separate longitudes decreases with increasing latitude. For Iceland, this effect is small or about 7%. However, whenever spatial distances needed to be calculated (e.g. the kriging interpolation) a norm that correctly reflected distances was used.

The altitude of each station is known, and the topographic map used to construct the linear model was obtained from the U. S. National Oceanic and Atmospheric Administration (NOAA) web server.¹ These data are shown in Figure 2.

Given a station location distance-to-open-ocean is known, i.e. its distance from a line that lies 10 km offshore from main peninsulas. A map of distance-to-open-ocean for each gridpoint is shown in Figure 3. In the study by Gylfadóttir (2003), the distance-to-coast was used instead of this predictand. However, subsequent analysis revealed a much stronger relationship between temperature variability at stations and their position with respect to open ocean. For instance, in the study by Bjornsson and Jonsson (2003) a clear difference was found in the annual cycle of temperature between coastal stations in NE Iceland that were located on the edge of peninsulas, and nearby stations that were located inside fjords. These stations differed in their distance-to-open ocean but not in their distance-to-coast.

The calculation of the eigenvectors of local topography is described in Bjornsson (2003). These predictands are meant to capture small scale topographic influence, and their use in the regression analysis is based on the method of Wotling et al. (2000). On the local scale, topography can be broken into various patterns. The eigenvectors are particularly useful for regression analysis because of their linear independence. The methodology for calculating the eigenvectors is fairly standard (Bjornsson and Venegas, 1997) and will not be described in detail in this report. The eigenvectors corresponding to the four dominant eigenvalues explain a combined 87% of the total local scale variance. These patterns correspond to a north - south slope, an east-west slope, a unimodal (hill/valley) feature and a saddle-like feature. The projections of these eigenvalues on the local topography are shown in Figures 4 and 5. These projections are

¹<http://www.noaa.gov/topography.html>

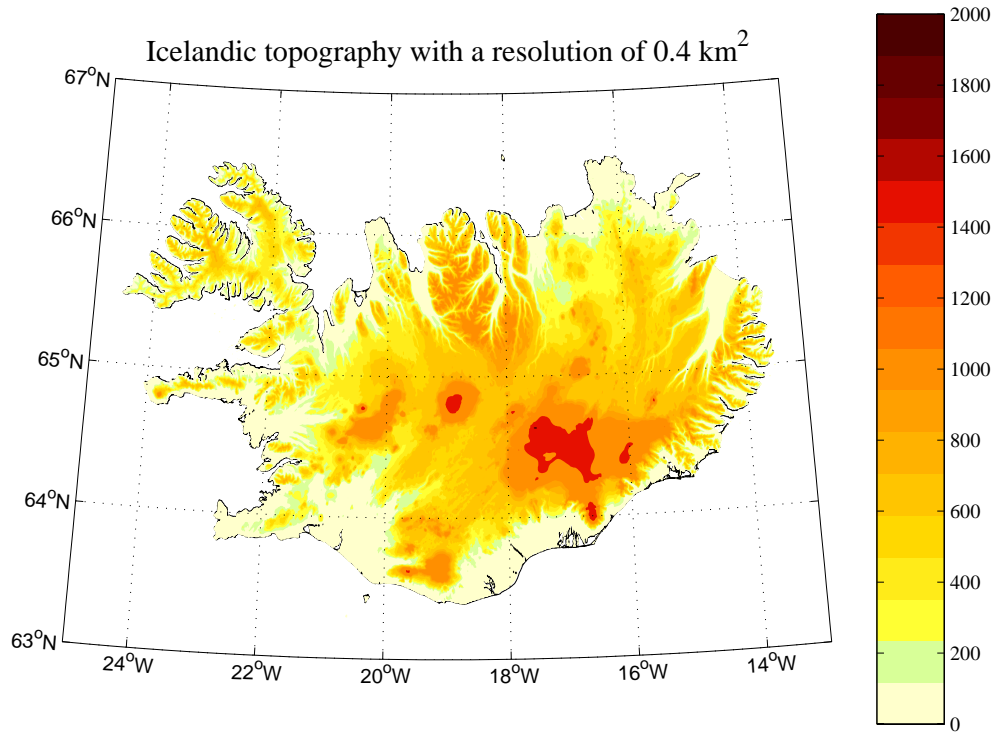


Figure 2: The topography of Iceland on a grid that is approximately 0.4 km^2 .

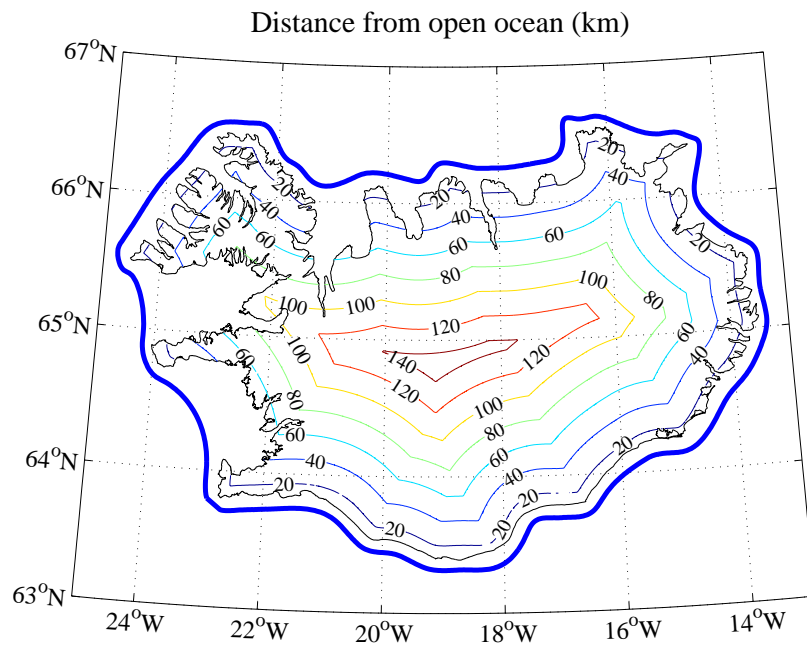


Figure 3: The distance to open ocean at any gridpoint on the map in Figure 2. The blue line corresponds to a line that is 10 km offshore from major peninsulas.

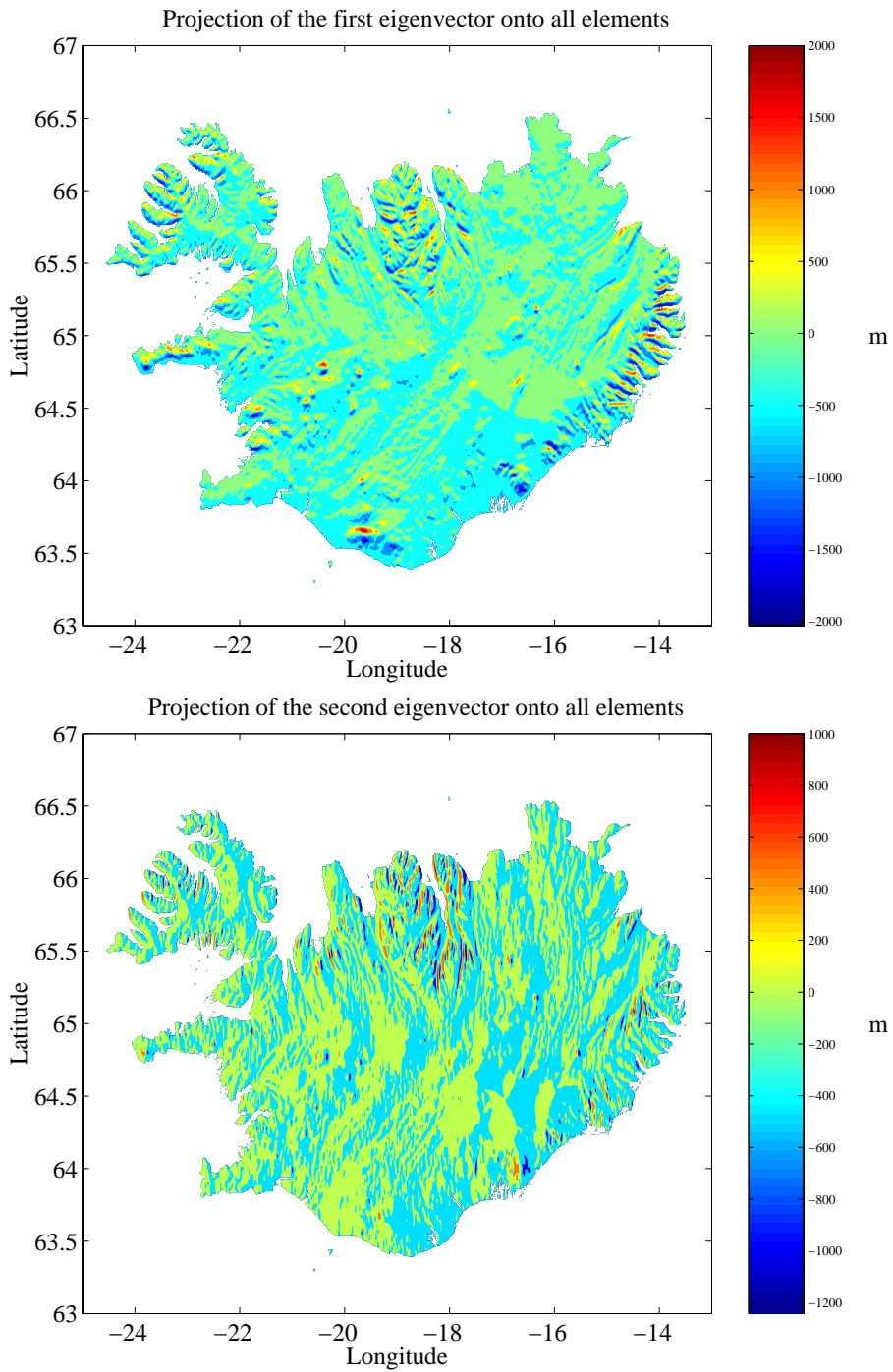


Figure 4: The projection of the first and second eigenvectors onto the local topography

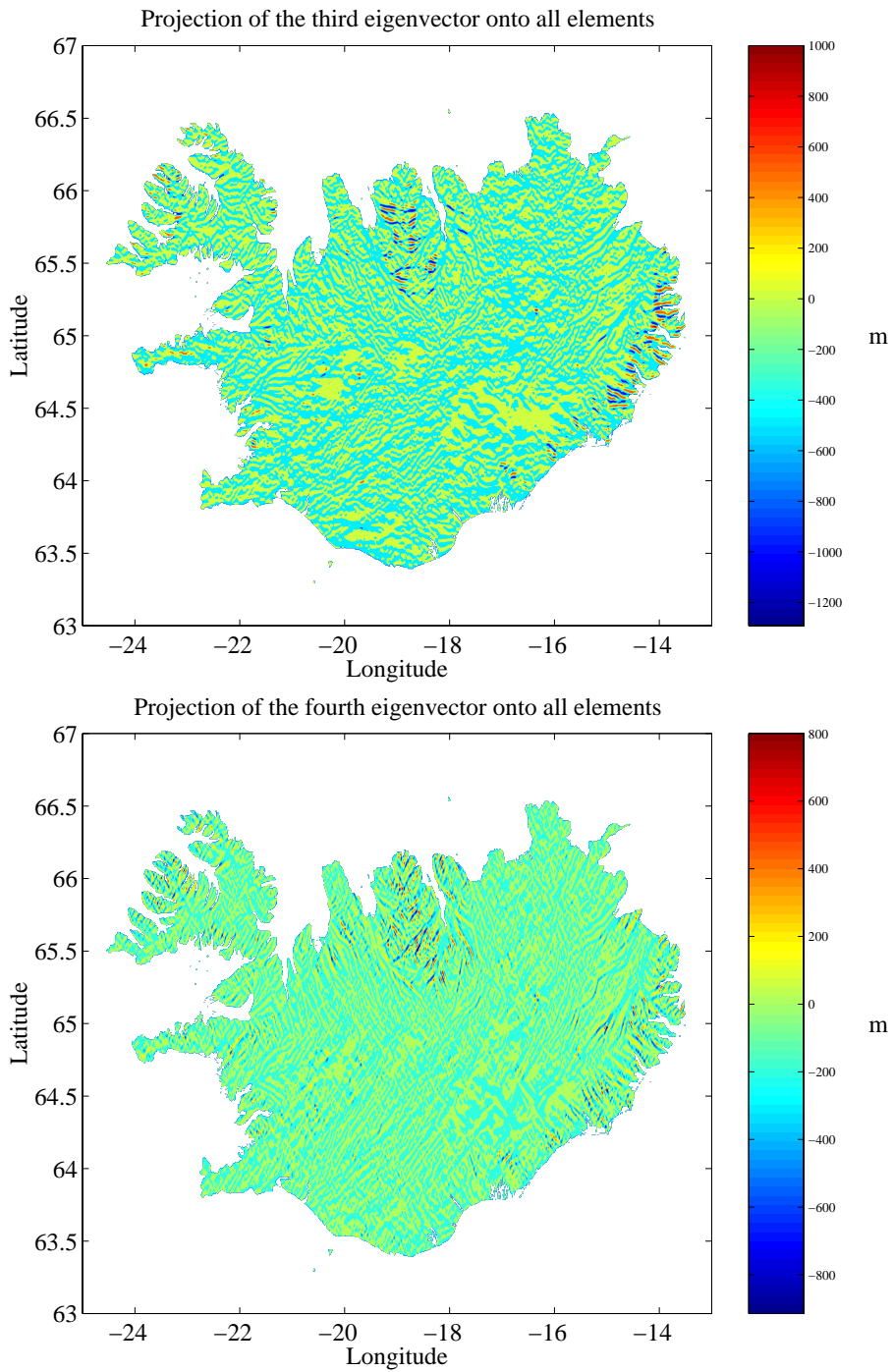


Figure 5: The projection of the third and fourth eigenvectors onto the local topography

used as the predictands EV_1 – EV_4 in the expression for T_l . To obtain these values for each station, the values from the maps in Figures 4 – 5 were read at the corresponding location. To ensure proper balancing of matrices that need to be inverted during the course of the linear regression it was found that the predictands needed to be normalized.

The station residuals (the difference between the station temperature and the linear model estimate) were then interpolated using the kriging method to produce the residual field R . The kriging method (Kitanitis, 1997) is a statistical interpolation method that uses all available data to evaluate the interpolated value at a chosen point, weighing it according to the distance from the point of interpolation. The weights are calculated using the semivariogram of the data. Kriging is exact, in that the interpolation produces the observed value at each station. The routines used here are partly based on those presented in Middleton (2000).

Results

The monthly mean temperature maps are shown in Figures 6 – 11, and the annual mean temperature is shown in Figure 12. To facilitate visual comparison the colorscale is kept the same in all the figures. During the middle of winter temperatures are below freezing throughout most of the country, with the exception of coastal areas in the south. During winter the average temperature in low lying areas (below 400 m altitude) ranges between 0°C and -3°C but for the country as a whole the average temperature is around -5°C . During summer, the temperatures in low lying areas range from 8 – 10°C , but the average for the country as a whole is around 7°C . It is apparent that in the northern part of the country, the cold season lasts longer and the warm season ends sooner.

How good are these estimates?

In order to estimate the uncertainties inherent in the method the following cross-validation was performed: A station was dropped from the sample, the above analysis was repeated and the value estimated at the station (T_{est}) was compared with the true value (T). Proceeding in this manner for all stations, an error-map for each month was constructed. Figures 13 and 14 show the results for January and July. The maps in the upper panel of the figures show that similar deviations do not “clump” together in certain areas, i.e., the deviations are spatially heterogeneous. The lower panels show the distribution of the deviations, and also a plot of T vs T_{est} . In both cases a typical error falls within $\pm 1^\circ\text{C}$. This magnitude of error is representative for all months (see Figure 15), for each month more than 90% of deviations have an absolute value less than 1°C .

It should be noted that the maps in Figures 6 – 11, and Figure 12 are calculated using the average altitude for each gridcell, which can differ from the altitude of a weather station situated within a gridcell. This height difference is usually small (typically less than 50m) but can lead to confusion if gridcell temperatures are compared to station temperatures.

One check for systematic errors in the temperature maps is to examine month-to-month differences in the maps and compare those to maps generated through direct kriging of differences calculated at the stations. Figure 16 shows an example of such a comparison. Here, the annual range, i.e., the January to July temperature difference was calculated from Figures 6a and 9a (“the model”) and also by kriging the January to

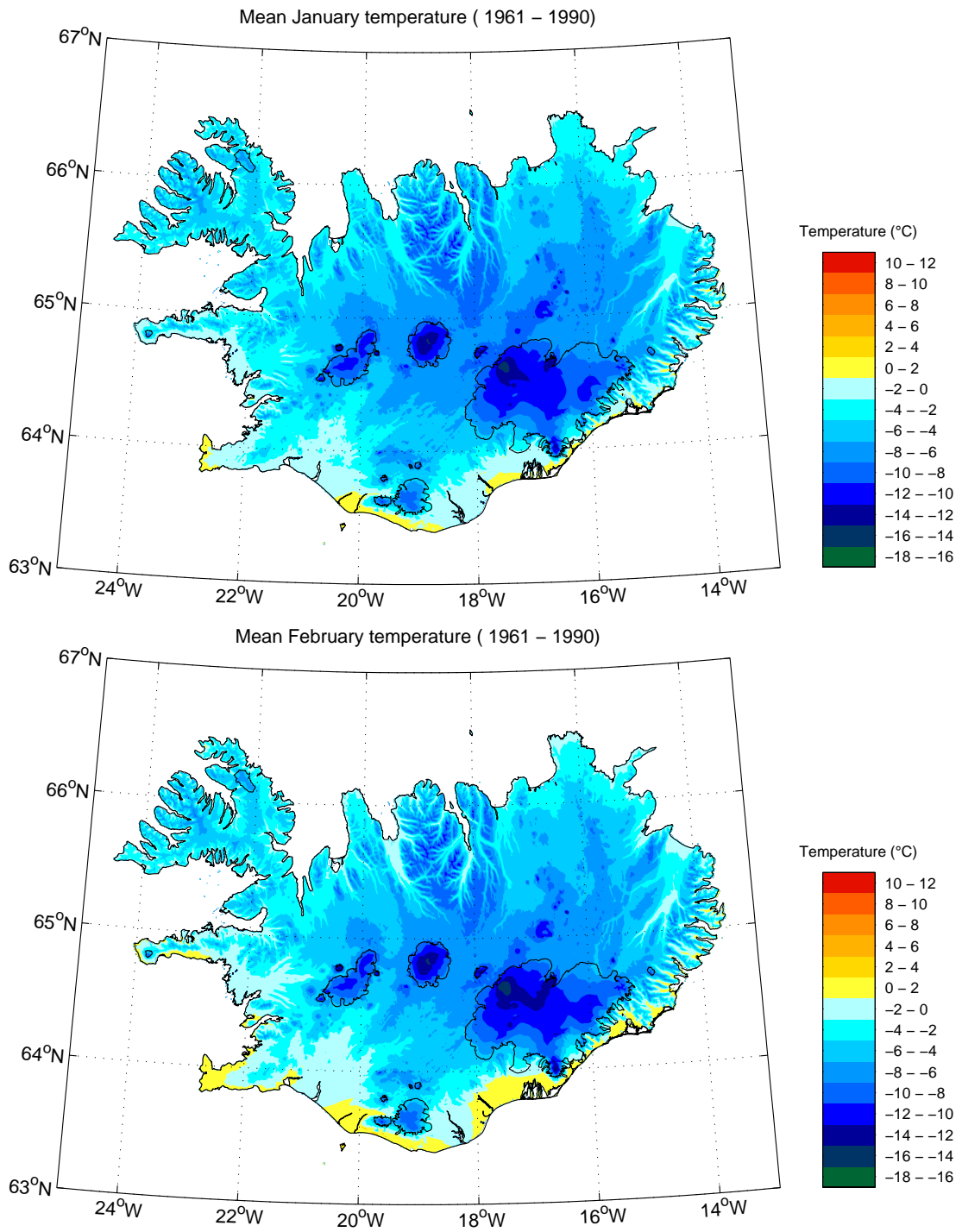


Figure 6: Maps of monthly mean (1961 – 1990) temperature. Results for January and February.

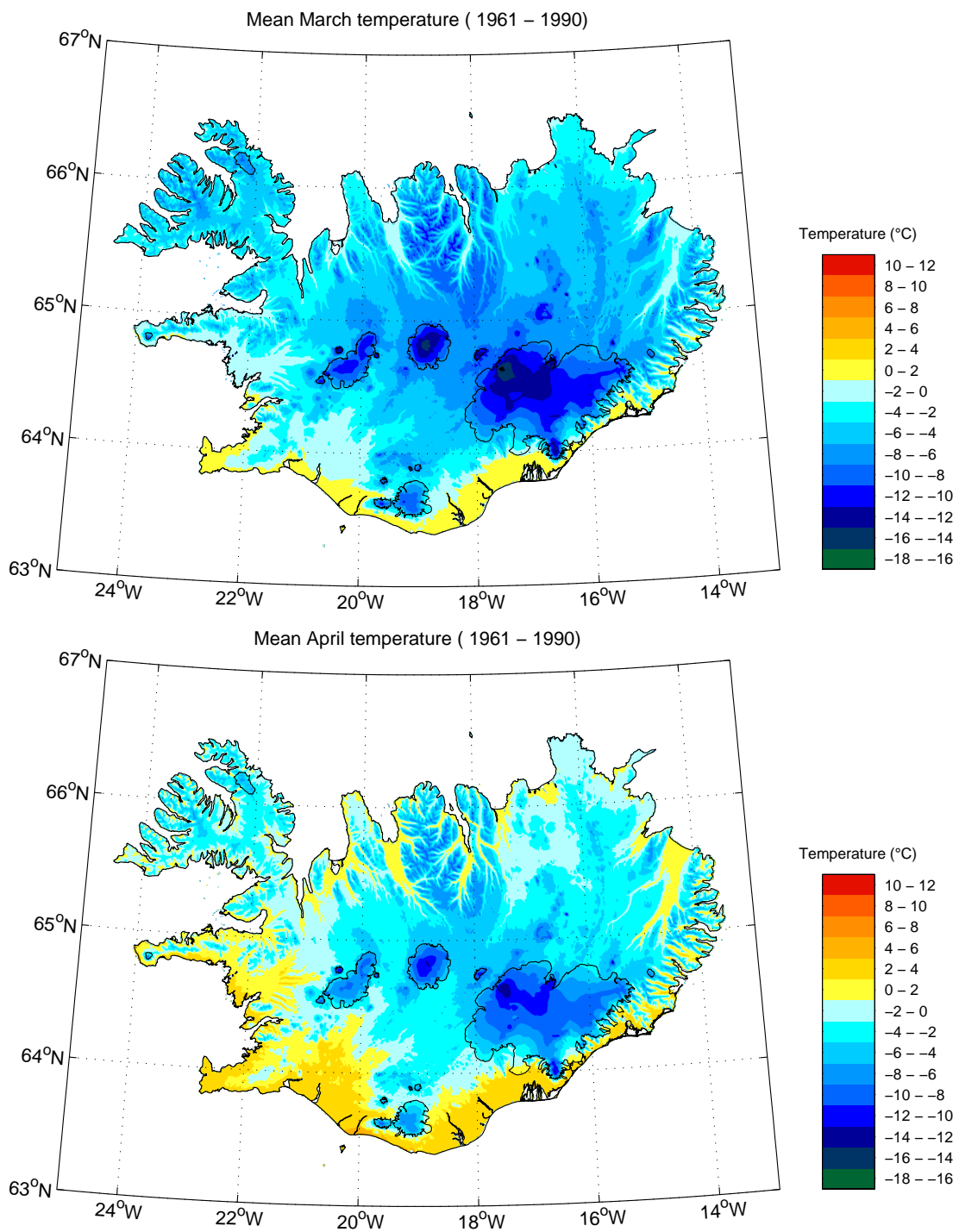


Figure 7: Maps of monthly mean (1961 – 1990) temperature. Results for March and April.

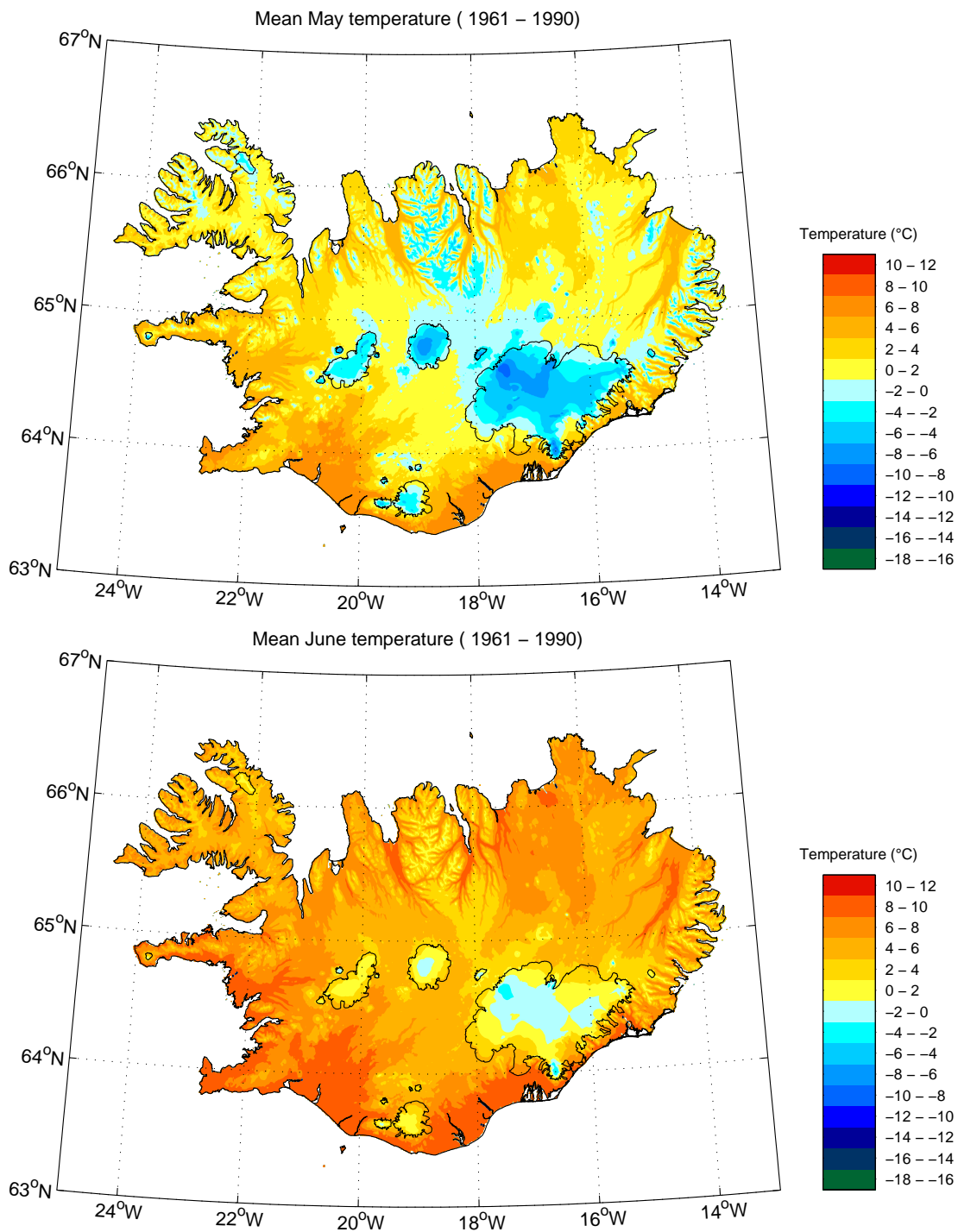


Figure 8: Maps of monthly mean (1961 – 1990) temperature. Results for May and June.

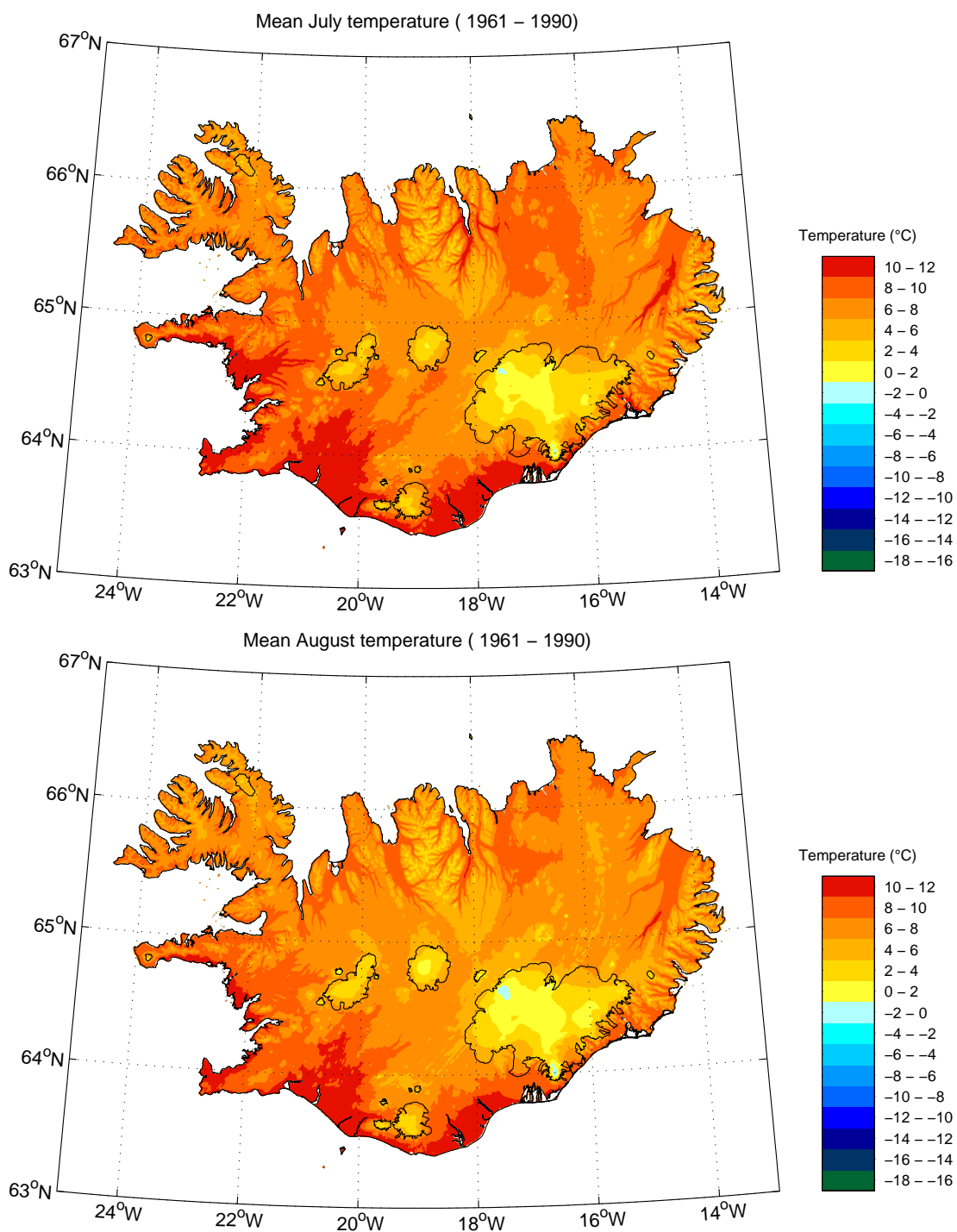


Figure 9: Maps of monthly mean (1961 – 1990) temperature. Results for July and August.

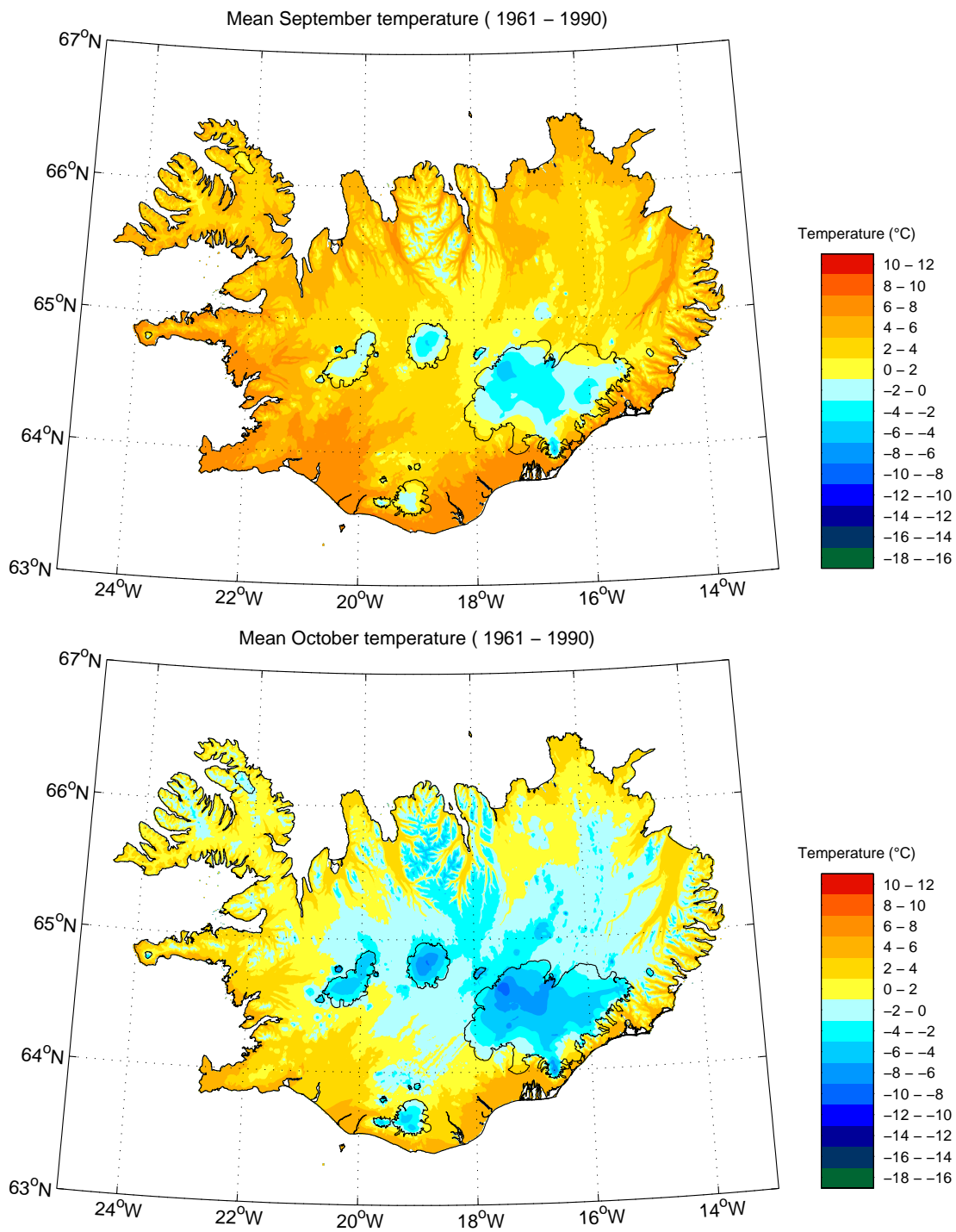


Figure 10: Maps of monthly mean (1961 – 1990) temperature. Results for September and October.

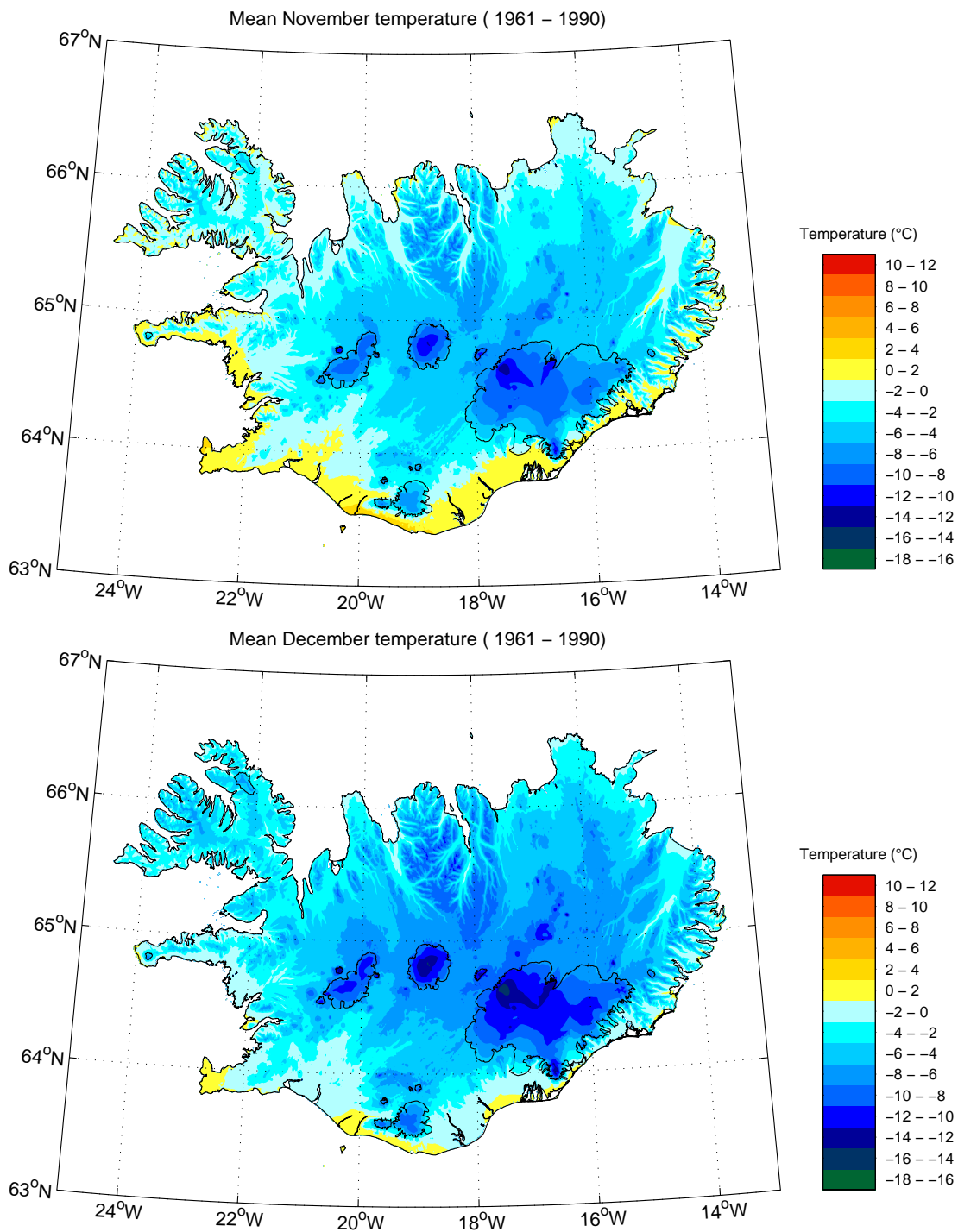


Figure 11: Maps of monthly mean (1961 – 1990) temperature. Results for November and December

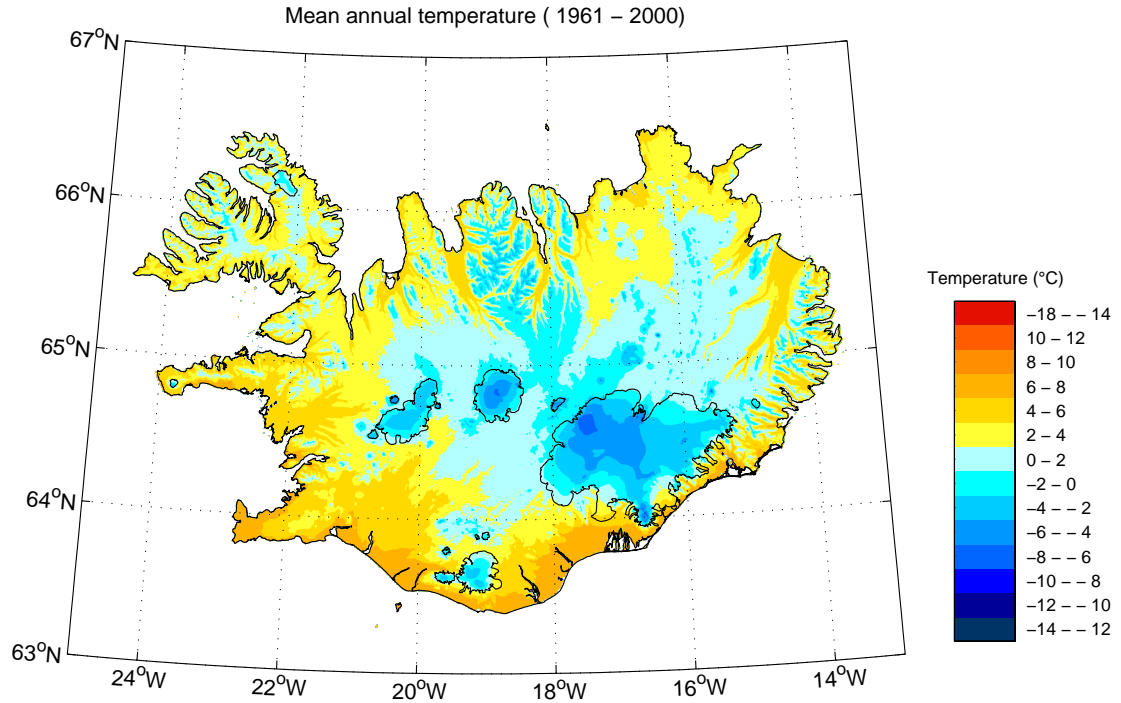


Figure 12: Map of mean (1961 - 1990) annual mean temperature.

July difference at each station (“the data”). While the two figures differ in detail, overall the resemblance is quite good. Especially, the location of maxima in the amplitude of the annual cycle is the same on both maps. The models used by Gylfadottir (2003) to produce monthly maps did not result in a model annual cycle that resembled the one obtained through kriging of the data. Indeed, it was this difference that led to the adoption of local eigenvector projection as predictands in the linear model.

The difference between the maps resulting from the two methods can be seen in Figure 17. It is clear from this figure that the annual range estimated by the model was larger than that obtained through direct kriging. The largest differences occur over glaciers, and over Trollaskagi (the largest peninsula on the north coast). The difference map for the temperature change from February to March was also calculated using the above methods, and the inter-method-difference was examined. While the magnitude was smaller, the spatial distribution of differences was similar, in that the largest differences occurred over Vatnajökull and Trollaskagi. Figure 18 shows the frequency distribution of the values in these two cases. Clearly the distribution for the annual range is similar to the distribution obtained for the cross validation (see Figure 15) but for the February to March temperature change, there is far less of a difference between the two methods. This is not surprising since the temperature change between the months is small in comparison with the annual range.

The results of the cross-validation indicate that the accuracy of the method is close to $\pm 1^\circ\text{C}$, which is somewhat larger than the error associated with a climatological monthly mean. The latter is used when comparing different 30 year intervals, and is estimated by using the sample variance of the 30 values that make up each 30 year

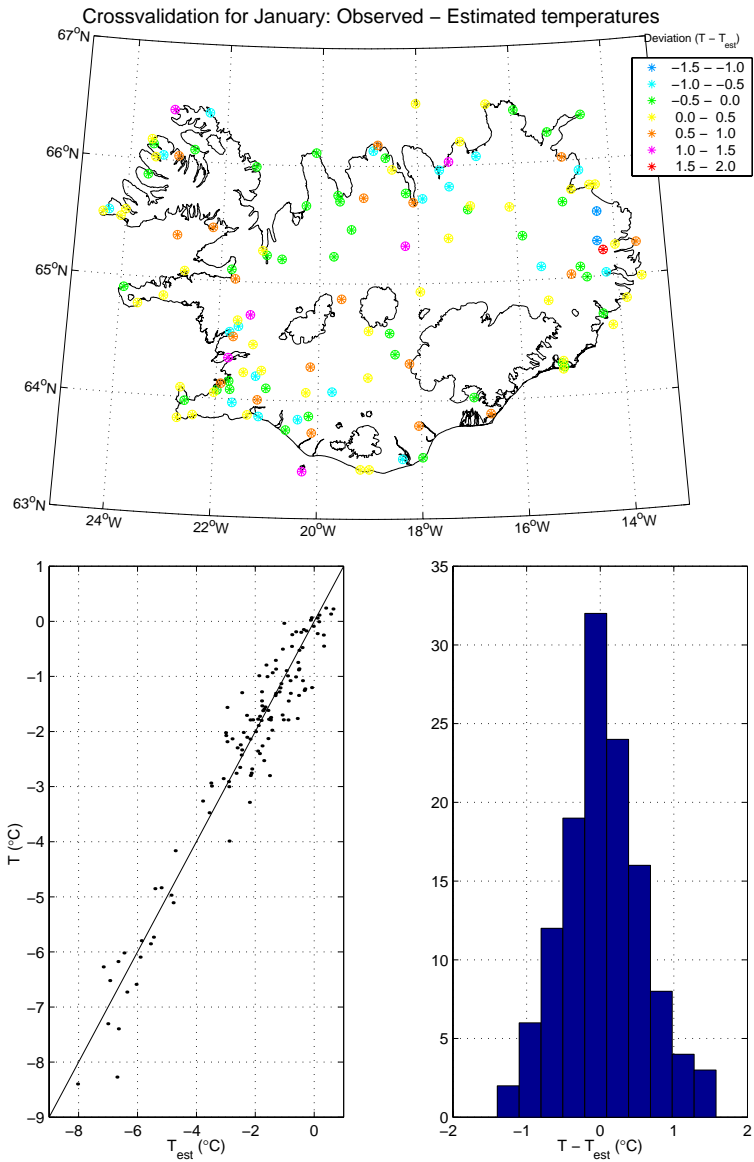


Figure 13: Cross-validation results for January. Upper: map of the deviations (observation, T minus estimate, T_{est}). Lower: A plot of observations vs. estimates and the distribution the deviations. The straight line is $y = x$.

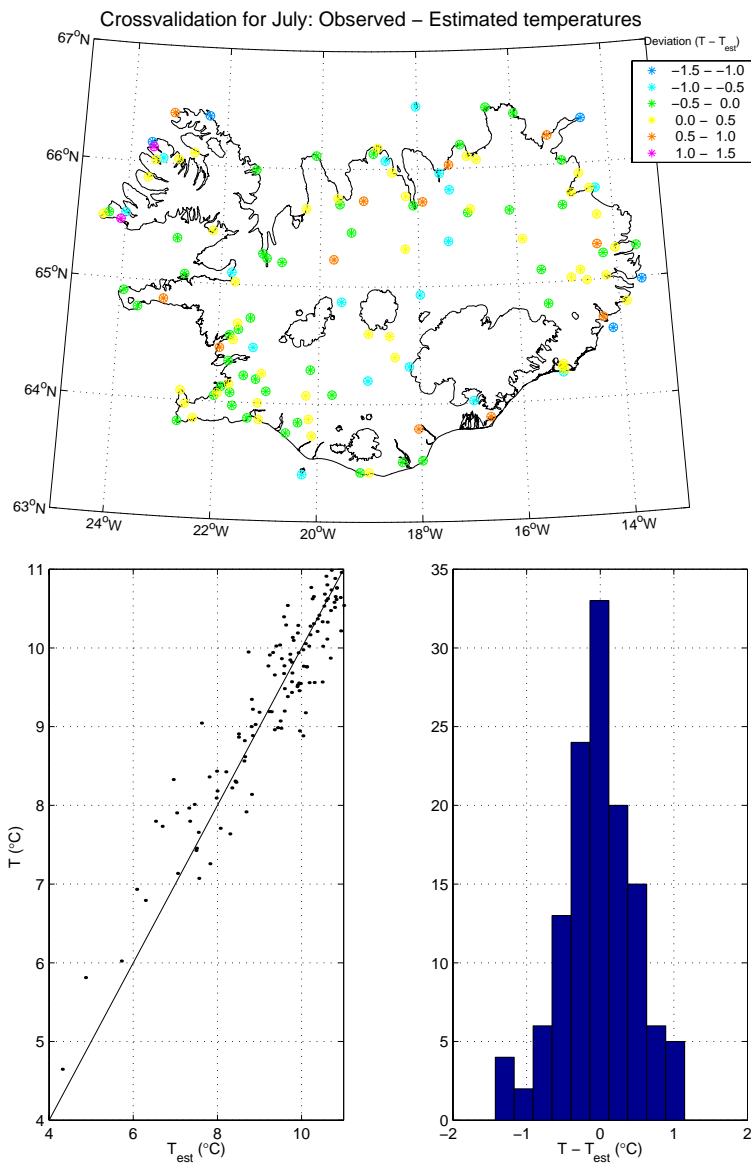


Figure 14: Cross-validation results for July. Upper: map of the deviations (observation, T minus estimate, T_{est}). Lower: A plot of observations vs. estimates and the distribution the deviations. The straight line is $y = x$.

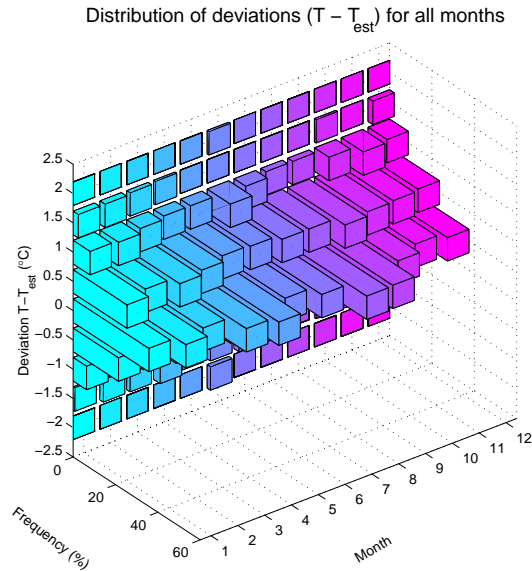


Figure 15: . The distribution of the deviations for all months.

monthly mean. The resulting confidence interval will vary from station to station and with season. However, typical values show that the 95% confidence interval for a 30 year monthly mean is $0.6 - 0.9^{\circ}\text{C}$ in the winter but $0.2 - 0.5^{\circ}\text{C}$ in the summer. With this in mind, the results of the cross validation procedure show an uncertainty which is acceptable.

The results of the above comparison are encouraging, but the spatial distribution of differences point to Trollaskagi and glaciers as areas of possible systematic errors in the method. It should be noted that applying kriging directly to the data, does not in itself produce the “true” map of temperature change, but the fact that the outcome of two methods differ, may be indicative of systematic errors. However, the fact that these are related to high altitude and glaciated areas is not surprising. While the adding the automatic stations did improve the network in mountainous areas, the highest station (Gagnheiði) is only at 949m. Furthermore, the method should be expected to fail over glaciated areas, especially during summer when the surface is at freezing, and cools down the surface air. This is an effect that is not included in the linear model, and there are no stations on the glaciers themselves to capture this effect.

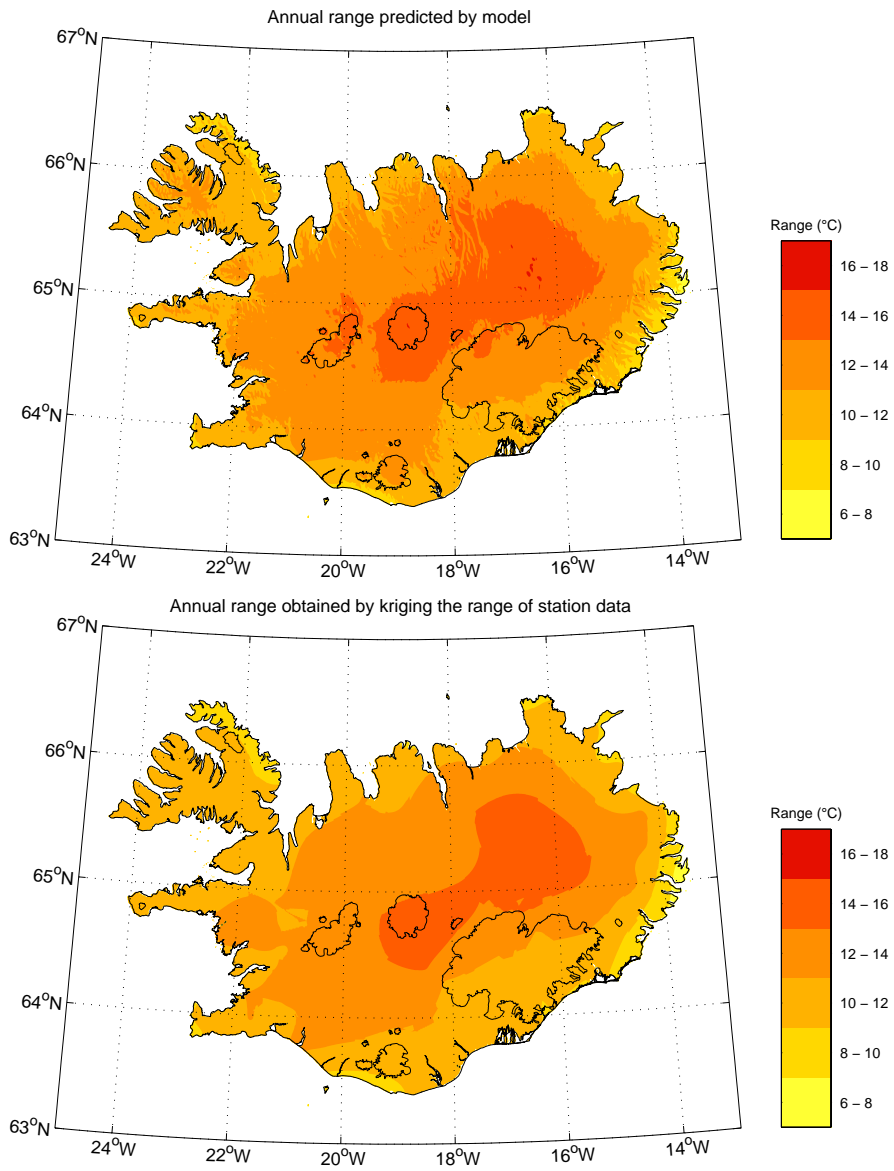


Figure 16: A comparison of the annual range obtained by using the difference of the maps in Figures 6a and 9a (“the model”) and that obtained by directly kriging the January to July difference at each station (“the data”).

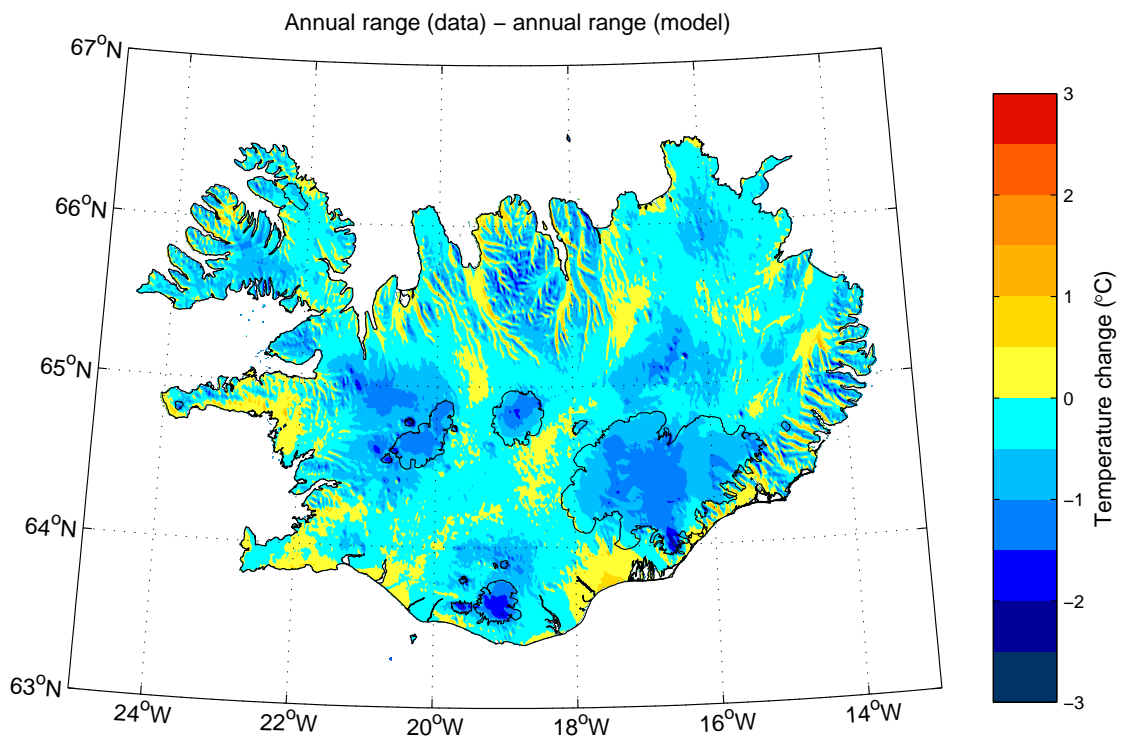


Figure 17: Inter-method differences. Upper panel: The difference between the maps in Figure 16.

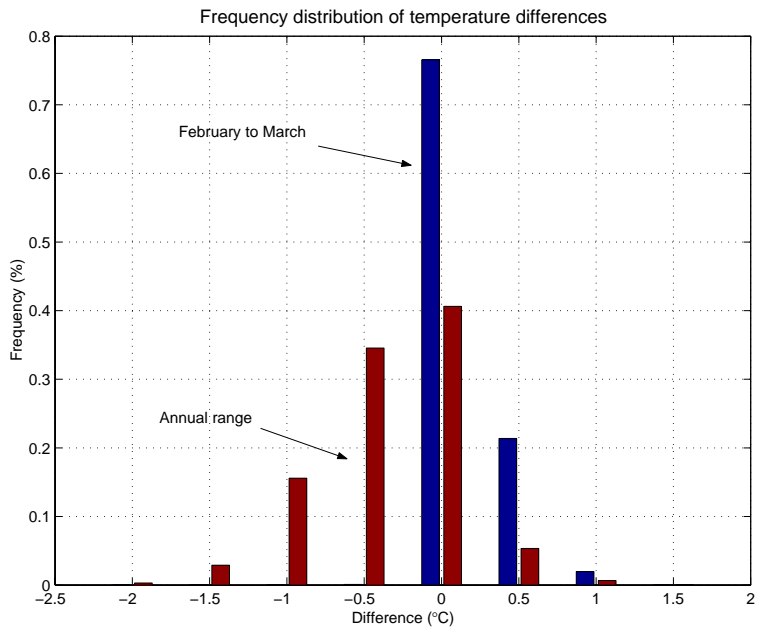


Figure 18: The distribution of inter-method-differences in from two methods for calculating the Annual range (see Figure 17) and the February to March temperature difference..

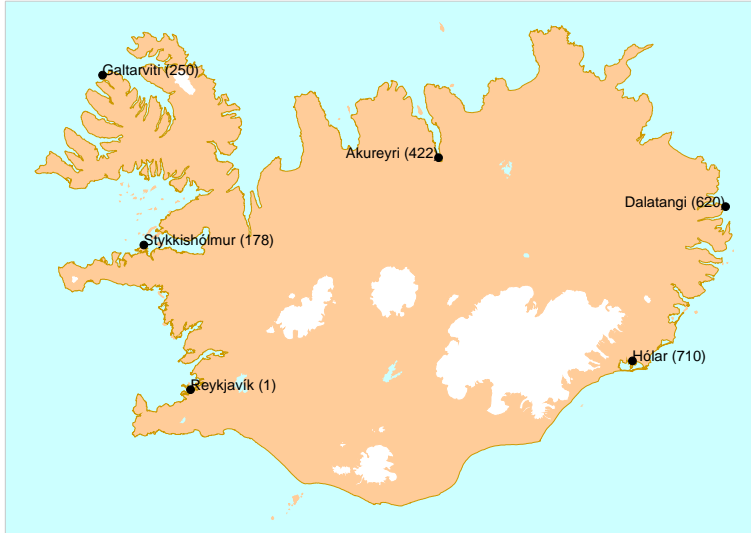


Figure 19: The location of the stations shown in figures 20. Shown are station name and number.

Interpolation to daily temperatures

With 12 monthly values at each gridpoint a smooth annual cycle can be obtained by interpolating the 12 monthly values to a 365 day year. The interpolation is done in a manner that preserves the monthly means, i.e., the average of the interpolated daily values in January is the same as the original January mean. Proceeding in this manner for all gridcells in the domain produced 365 maps of temperature. These maps were then used to calculate daily counts and related indices.

Method

The method used is described in detail in Henriksen (2003a) and applications can be found in Henriksen (2003b). Similar calculations that were done for the Nordic Countries and published by the Nordklim group (Tveito et al., 2001) used cubic spline for the interpolation, with a slight modification to preserve monthly means. For the Icelandic data it was found that cubic splines exaggerated the maxima and minima of the annual cycle in an unrealistic fashion, and thus Henriksen (2003a) used a modified tension-spline method for the interpolation. As in the Nordic Maps the modification ensured that monthly means were preserved. This led to a non-linear optimization problem and a “smart” search algorithm had to be written to find the best solution. The method can be applied to station data and plotted against daily means for the reference period. Figure 19 shows the location of six stations that have been interpolated with tension splines and the results of the interpolation are shown in Figure 20.

The results in Figure 20 show clearly the main features of the annual cycle in temperature. The temperature curves are relatively flat during a cold season that extends from December to March. Following that there is a rapid rise in temperature from April to June, but the temperature levels off during the summer season. In the fall, temperatures decrease rapidly until the cold season is reached again. This behavior with two relatively “flat” intervals and a ramp-up or ramp-down can be explained in

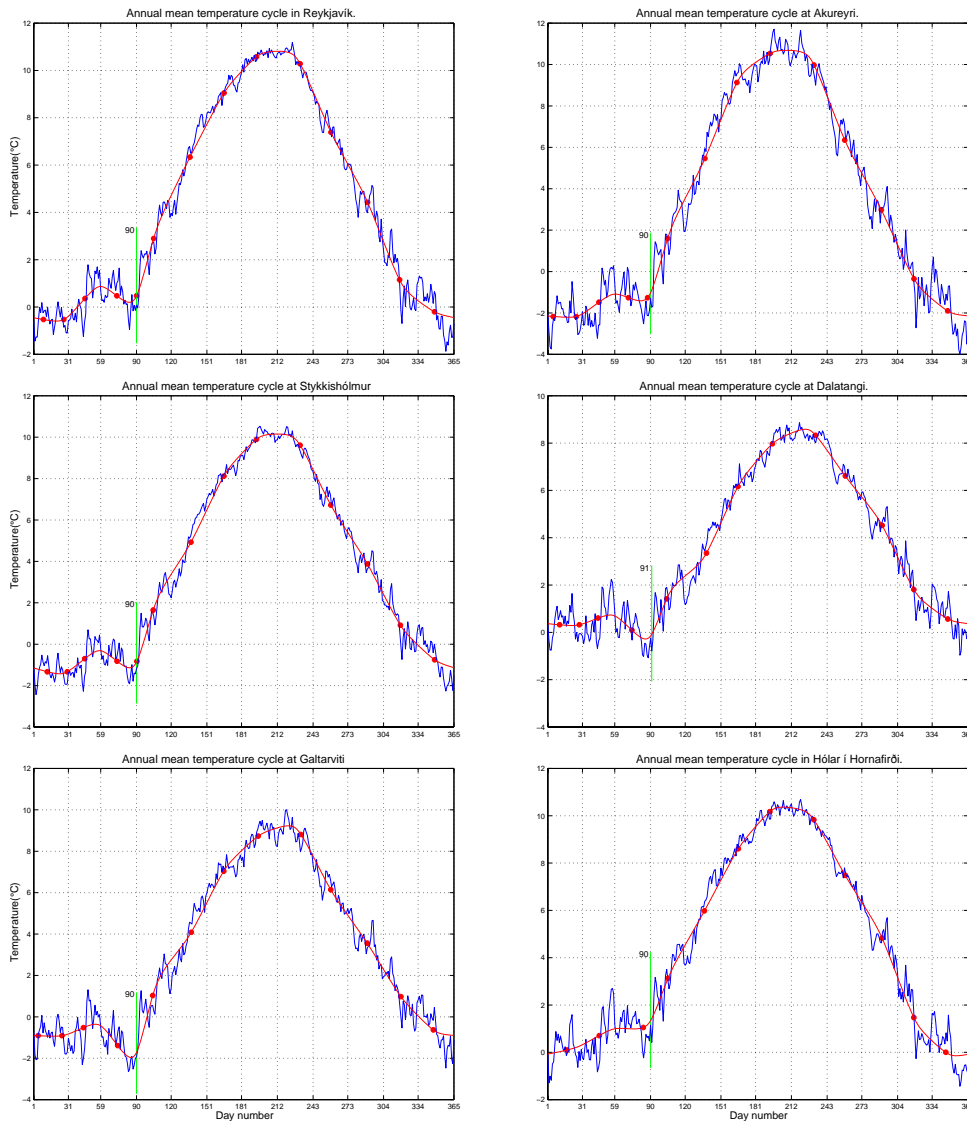


Figure 20: Results of modified tension spline interpolation to monthly means (smooth curve). Also shown are the daily means for the reference period (broken curve). The points show the monthly mean, and they are placed on the day when the daily temperature reaches the monthly mean (this may happen twice during the same month). The vertical line marks the day when the slope of the smooth curve reaches the average slope between the March minimum to the July/August maximum. The position of this line represents a measure of the onset of spring warming.

terms of the moderating influences of the ocean around Iceland. During winter the ocean loses heat to the atmosphere and keeps winter temperatures rather mild, and during summer the ocean absorbs heat from the atmosphere and places limits on how warm the summers get. It was this behavior that led to the adoption of tension splines instead of cubic splines since the latter could not properly reproduce the “flat” periods, but instead produced significant excursions from the daily means.

One feature that increases the complexity of the seasonal cycle in these figures is the persistent second minimum that occurs in March. The naive view of annual cycle is one where a minimum occurs around January and each month thereafter experiences warming on the previous month (until late summer). However, in many locations in Iceland, February will be warmer than January, but March will be colder than February. The spatial distribution of this “double dip” behavior can be seen in Figure 21. These

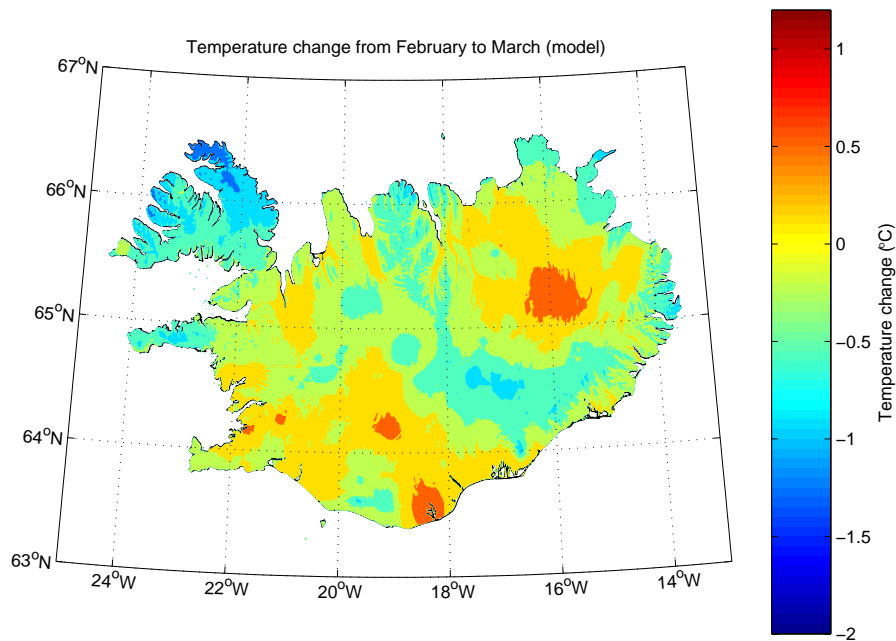


Figure 21: The change in temperature from February to March. Shown are results obtained by taking the difference of the maps in in Figures 6b and 7a.

results show March being colder than February in an area that roughly extends from Snæfellsnes peninsula on the west coast of Iceland to the north west peninsula where the amplitude of the March cooling is strongest. The area then extends along peninsulas on the north coast to the fjords on the east coast of Iceland. The reason for the “double dip” is not completely clear, but this signal is not a permanent feature of Icelandic climate records, but seems to have been fairly strong in data from the 1961 - 1990 period (Henriksen, 2003b).

The tension spline interpolation method was then used to interpolate each gridpoint in the 12 monthly maps of Figures 6 to 11. Following this various daily counts could be calculated at each gridpoint and mapped spatially.

Results

Length of periods with T greater than a given threshold value

The number of days per year when the temperatures reach or exceed 0°C and 7°C can be seen in Figure 22. Clearly, along the south shore, the estimated duration of the period with mean temperature above freezing is longest, whereas it is shortest on glaciers. For higher temperature thresholds fewer days are counted in the highlands and along the northern coast.

It should be kept in mind that maps of this kind are inherently biased. To appreciate this consider a location where the mean temperature never rises above 6.95°C . Using a threshold value of 7°C would yield a count of zero as the number of days where temperature exceeds the threshold. But in reality, during the warmest part of the year, close to half of all days will have temperatures that exceed 7°C , and thus the average number of days with temperature exceeding the threshold should be greater than zero. Likewise, if the minimum average temperature is 0°C the above method would yield a count of 365 days for all threshold values less than zero. But during the cold season there must be several days with subzero temperatures to yield an average of zero. Thus, the method would overestimate the count for threshold values of -1°C , -2°C , etc. The overestimate would become less severe with decreasing threshold values as the occurrence of days below the threshold decreases.

Figure 23 shows the mean number of days temperatures exceed threshold values ranging from -20°C to 20°C calculated using daily data, and using the mean annual curves. The figure shows results for Reykjavik and Akureyri, but similar results hold for any other location in Iceland. They clearly show that there is a large discrepancy between the two methods. The difference is less severe if threshold values are limited to range between the maxima and minima of the mean curve (approx. 9°C and 11°C , respectively). This means that the maps in Figure 22 have to be “handled with care” since they are likely to be biased, especially the upper one. Duration maps such as these need to be corrected if they are to be used for serious applications. In the next section degree day maps are calculated. As these will be used for various applications the bias will be discussed in detail and maps will be corrected.

Biased degree-day maps

Measures related to those shown in Figure 22 are the degree days above a certain threshold. For a chosen temperature threshold, the degree day value is the sum of all positive temperature anomalies above the threshold. Here, *anomaly* means the temperature minus the threshold value. Using mean annual curves, this method has been applied by the Nordklim group to produce degree-day maps for the Nordic countries (Tveito et al., 2001). As is explained in the previous section, this method is not unbiased and the bias will be examined in detail below. Figure 24 shows the results obtained by calculating the degree days with 0°C as threshold, and also results for threshold values of 5°C and 10°C . The ten-degree day map shows low values over most of Iceland. Values exceeding 50 only appear in low lying areas mainly on the south coast.

Examining the maps in Figure 24 it is important to keep in mind that these are calculated from an average annual cycle. By construction, these bias calculated degree day values. To appreciate the definition of degree days must be examined. For a period starting with julian day d_1 and ending on julian day d_2 (in the maps above $d_1 = 1$ and $d_2 = 365$ were used) and a threshold value K , the N -year average degree day value is

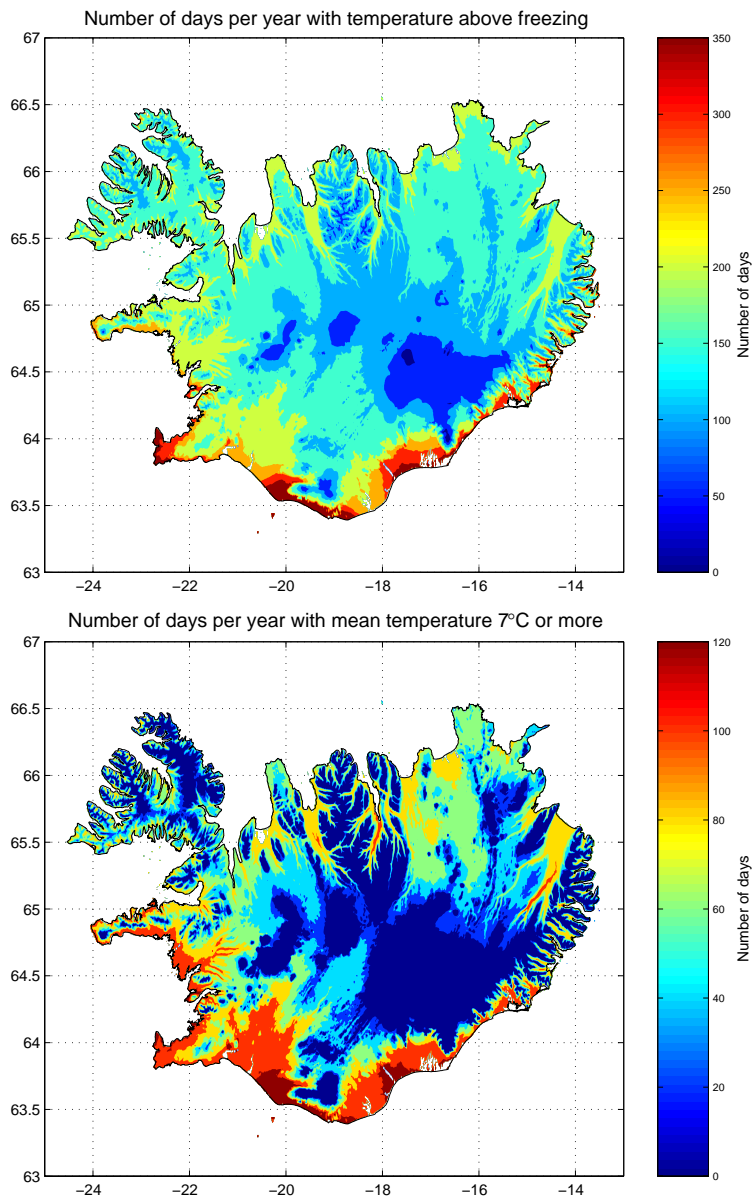


Figure 22: The number of days per year with temperature equal to or above 0°C (upper panel) and 7°C (lower panel).

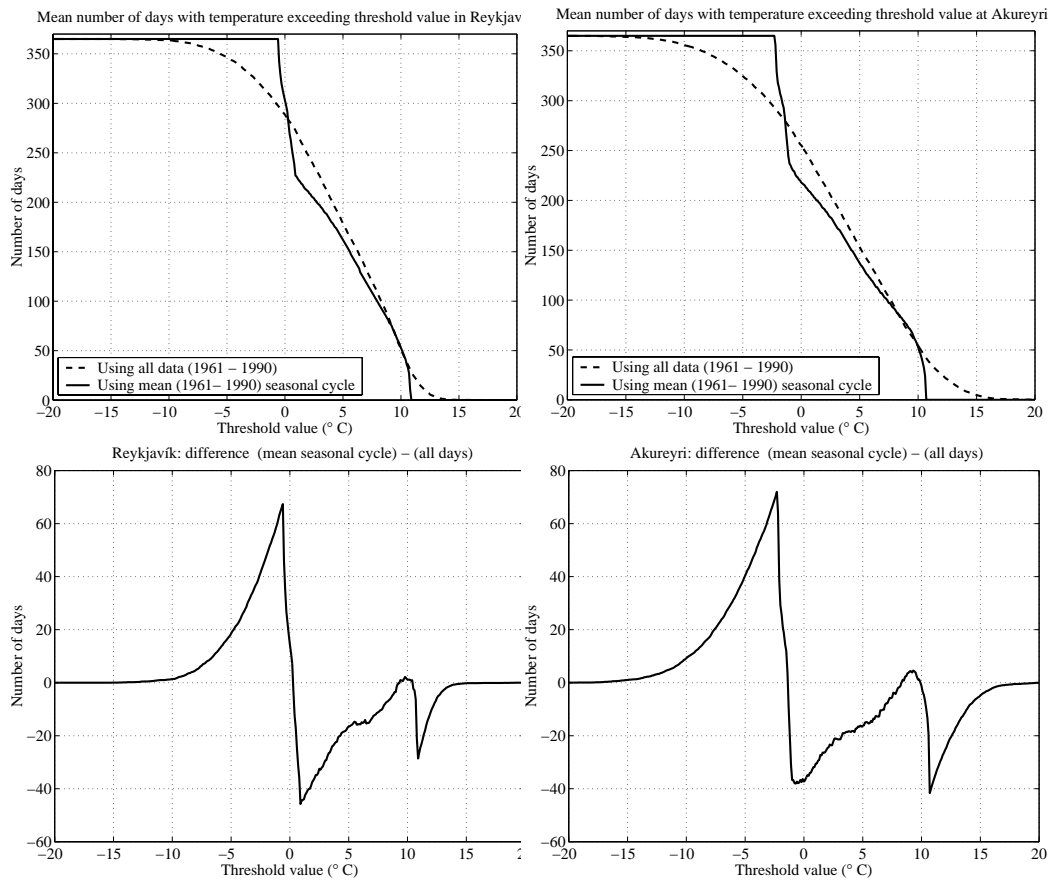


Figure 23: Differences between calculating the mean number of days with temperature exceeding a given threshold by using daily temperature data, and by using the mean annual curves.

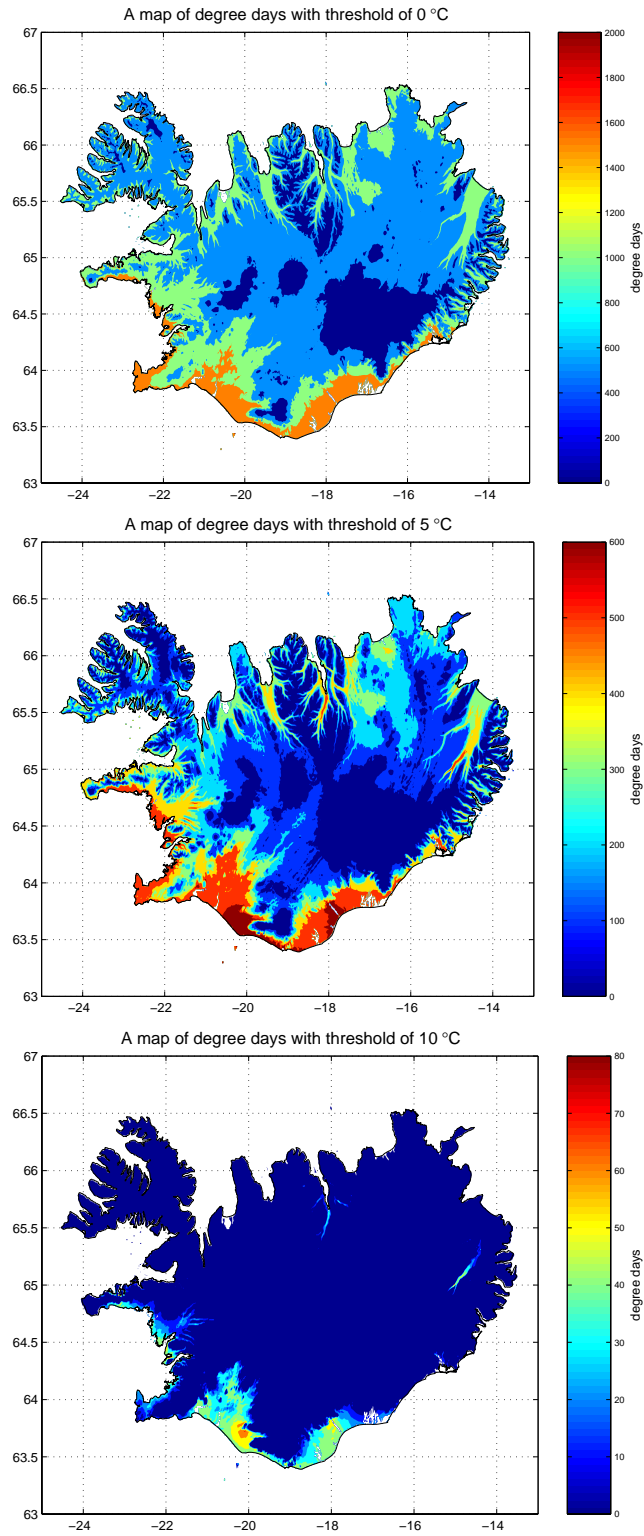


Figure 24: Biased degree day maps with thresholds of 0°C, 5°C and 10°C.

given by:

$$\overline{DD} = \frac{1}{N} \sum_{i=1}^N \sum_{d_1}^{d_2} (T_{i,j} - K) H(T_{i,j} - K),$$

where $T_{i,j}$ is temperature on day j , year i and $H(T_{i,j} - K)$ is the Heavyside function ($H(T_{i,j} - K) = 0$ if $T_{i,j} < K$ but 1 otherwise).

The contribution of one day $d_1 = d_2 = d$ to \overline{DD} is

$$\overline{DD}_d = \frac{1}{N} \sum_{i=1}^N (T_i(d) - K) H(T_i(d) - K),$$

where $T_i(d)$ is the temperature of day d on year i . Now write $T_i(d)$ as

$$T_i(d) = M(d) + \varepsilon_i,$$

where $M(d)$ is the N year average of the temperature

$$M(d) = \frac{1}{N} \sum T_i(d),$$

and ε_i is the departure from the mean for year i . With this \overline{DD}_d can be written as

$$\overline{DD}_d = \frac{1}{N} \sum_{i=1}^N (M(d) - K + \varepsilon_i) H(M(d) - K + \varepsilon_i).$$

The mean temperature-to-threshold difference can be written $S = M(d) - K$ and the contribution becomes

$$\overline{DD}_d = \frac{1}{N} \sum_{i=1}^N (S + \varepsilon_i) H(S + \varepsilon_i),$$

but this can be written as

$$\overline{DD}_d = \frac{S}{N} \sum_{i=1}^N H(S + \varepsilon_i) + \frac{1}{N} \sum_{i=1}^N \varepsilon_i H(S + \varepsilon_i).$$

If $F(\varepsilon_i \geq -S)$ is fraction of days that $\varepsilon_i \geq -S$, i.e., the fraction of days the Heavyside function is “turned on”². and the mean of the temperature departure for the times when $\varepsilon_i \geq -S$ is

$$\eta_S = \frac{1}{N} \sum \varepsilon_i H(S + \varepsilon_i),$$

the unbiased expression for the degree-day contribution becomes

$$\overline{DD}_d = S \cdot F(\varepsilon_i \geq -S) + \eta_S$$

The Nordklim method, used to generate the maps in Figure 24 used simply the (positive) mean temperature-threshold difference as \overline{DD}_d ,

$$\overline{DD}_d = SH(S).$$

²This can be seen by noting that

$$F(\varepsilon_i \geq -S) = F(\varepsilon_i \geq K - M(d)) = F(M(d) + \varepsilon_i \geq K) = F(T(d) \geq K).$$

Clearly the two methods differ considerably. The Nordklim method has an “on-off” character to it. Either a day is counted fully or it does not count at all. In the unbiased expression the same term is weighted with an appropriate fraction. Furthermore there is an extra term in the unbiased expression which can become larger than the first term when the threshold value (K) is close to the mean value of the day ($M(d)$). Indeed, the only cases where the two methods agree is when $F = 1$ or when $F = 0$. In the first case $S \gg |\epsilon_i| \forall i$ and thus $H = 1 \forall i$. In this case the Nordklim method yields $\overline{DD}_d = SH(S) = S$ and the full expression yields

$$\overline{DD}_d = \frac{SN}{N} + \frac{1}{N} \sum_{i=1}^N \epsilon_i = S,$$

since $\sum_i \epsilon_i = 0$, which is the same result. In the latter case both methods yield $\overline{DD}_d = 0$.

To gain an appreciation of this the terms in the unbiased expression will be examined in more detail.

1. The first term, $S \cdot F(\epsilon_i \geq -S)$, will be negative if $K > M(d)$, but positive if $K < M(d)$. Starting with a low threshold value, say $K = -20^\circ\text{C}$, S will be positive and furthermore $F = 1$ for most days of the year. If K is then increased the fraction F will go down, as will S . Once K has reached the mean value ($M(d)$) this term will be zero. When K is increased further the term becomes negative and S remains negative for further increases in K but its absolute value becomes larger. However, despite this the term usually remains close to zero, because F approaches zero as K increases.

If $\rho(\epsilon)$ is the distribution of the random variable ϵ (the ϵ_i values are different realizations of this random variable) then

$$\lim_{N \rightarrow \infty} F(\epsilon_i \geq -S) = \int_{-S}^{\infty} \rho(\epsilon) d\epsilon.$$

Simplifying assumptions can be made about $\rho(\epsilon)$, e.g. that it is Gaussian, and this expression can be used to obtain the expected value of the fraction $F(\epsilon_i \geq -S)$ given S . Such assumptions are made in methods that estimate degree days directly from monthly means and average standard deviations within months (Braithwaite, 1984).

In summary, the first term is a large positive number when K has a very low value, it goes to zero as K approaches $M(d)$ and becomes negative but remains small for K larger than $M(d)$. For large enough K the term tends to zero.

2. The second term, $\eta_S = \frac{1}{N} \sum \epsilon_i H(S + \epsilon_i)$, is the mean of the temperature departure for the times when $\epsilon_i \geq -S$. To gain an understanding of this term it is instructive to sort the departures ϵ_i in an ascending order and write them as

$$\{\epsilon_A, \epsilon_B, \epsilon_D, \epsilon_E, \dots, \epsilon_L, \epsilon_a, \epsilon_b, \epsilon_d, \epsilon_e, \dots, \epsilon_l\}$$

where negative departures have underscores with capital letters. The term can be written as

$$\eta_S = \text{sum}\{\dots\}/N,$$

where “sum” denotes the summation function of the list $\{\dots\}$ and N is the number of years in consideration. The number of items in the list depends on the threshold value K , the larger the threshold value, the fewer items are in the list.

The behavior of this term can be understood by focusing on how many items remain in the list for a chosen K . Starting with a threshold value that is low enough so that $H(S + \varepsilon_i) = 1 \forall i$, then all the ε 's are in the list and $\eta_S = \frac{1}{N} \sum \varepsilon_i = 0$. When the threshold value is increased sufficiently the lowest value in the list (ε_A) is thrown out, and as this value is negative the sum becomes positive. As K is increased further more items (all negative) are thrown out of the list so the sum increases further. It follows, that the term grows with increasing K until the threshold value equals the mean temperature ($K = M(d)$ i.e, $S = 0$). In that case only positive temperature departures remain in the list and

$$\eta_S = \text{sum}\{\varepsilon_a, \varepsilon_b, \varepsilon_d, \varepsilon_e, \dots, \varepsilon_l\} / N.$$

This is the threshold value of which η_S is largest. Further increases in K eventually lead to positive items being thrown out which reduces the sum. Eventually all items have been thrown out of the list and $\eta_S = 0$. In summary, the second term is zero when K is a large negative number or when K is a large positive number. In between the term is positive, reaching a maximum value when $K = M(d)$.

Figure 25 shows a comparison of the Nordklím method and a direct calculation for the N -year average contribution of one day (\overline{DD}_d) to the degree day sum (\overline{DD}) for a given threshold. The calculations were done with data from Akureyri using daily data from 1961 to 1990. The figure shows two particular days, January 15th (cold) and July 20th (warm). The figure also shows the contribution of the two terms that \overline{DD}_d be broken into. Notice that for January 15th the Nordklím method yields zero \overline{DD}_d for all thresholds, but direct calculation reveals that \overline{DD}_d is nonzero for thresholds below 6°C . For July 20th the method works better, significant bias only arises when the threshold value exceeds 8°C .

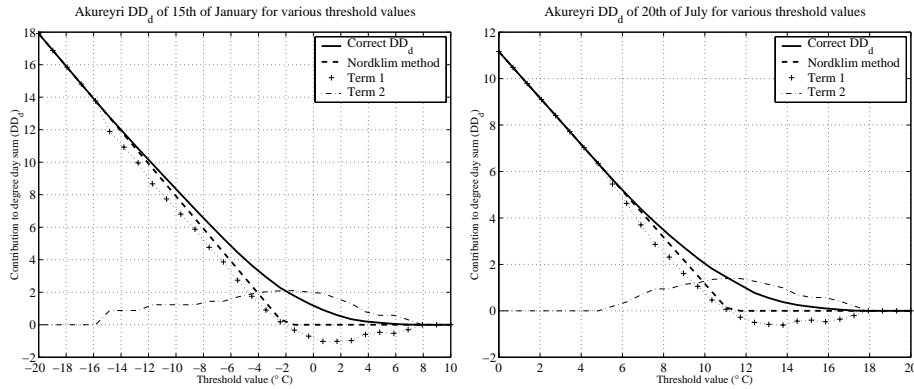


Figure 25: A comparison of the Nordklím method and a direct calculation for calculating the N -year average contribution of one day (\overline{DD}_d) to the degree day sum (\overline{DD}) for a given threshold. Shown are two days, January 15th (cold) and July 20th (warm) at Akureyri using daily data from the period 1961 to 1990. The figure also shows the contribution of the two terms that the unbiased \overline{DD}_d can be broken into.

Figure 26 shows the results of a direct comparison for the whole year for Reykjavík and Akureyri using daily data from 1961 to 1990, and the mean annual curves. Threshold values from -20°C to 20°C are used. The differences between the two methods are less striking than for the number of days temperature exceeded a threshold value shown

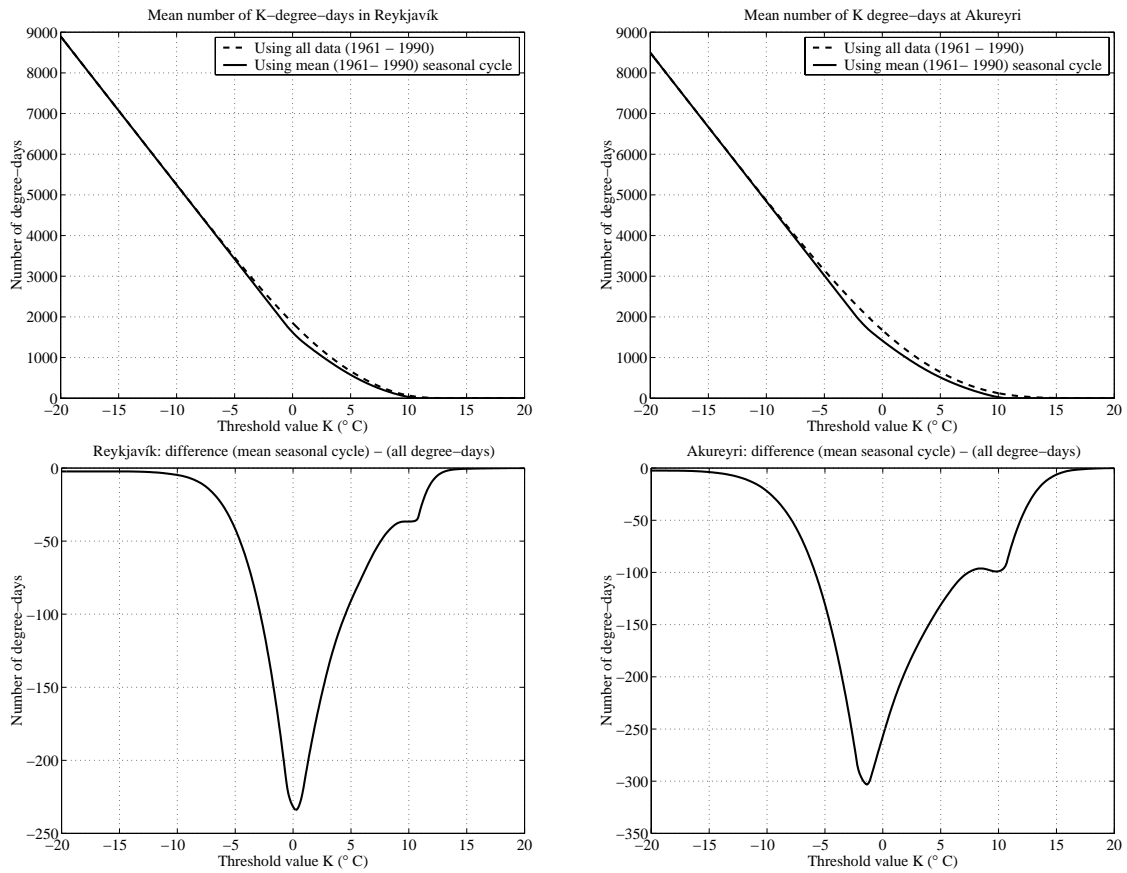


Figure 26: Differences between calculating the degree-day number with by using daily temperature data (from 1961 – 1990), and by using the smooth daily mean curves.

in Fig. 23. When the threshold value lies outside the range of the mean annual curves, the two methods tend to compare fairly well. However, there are significant differences when the threshold value lies within the range of the mean annual curves. Since this range (c.a. 0°C to 11°C) marks reasonable threshold values these differences do pose a problem and special methods must be devised to correct maps made with temperature thresholds in this range.

Corrections to the map bias

A method to correct the bias is described in Ólason (2003). First correct degree day values are calculated at 50 stations. Next the smooth daily curves calculated for the station using the method of Henriksen (2003a) are shifted by a factor ϕ so that the degree day calculation using the Nordklím method gives the correct value. With this change the expression for degree days for the whole year becomes

$$DD(\phi) = \sum_{d=1}^{365} (m_d + \phi - K) H(m_d + \phi - K),$$

where m_d is the smooth mean daily temperature curve, and K is the threshold value. The ϕ field was then interpolated to a map and added to the temperature data, and following that the Nordklím method to calculate the degree days was applied.

To interpolate ϕ to a grid it was written as

$$\phi = a_o + a_1 \cdot L_x + a_2 \cdot L_y + R,$$

where the a_i are constants, L_x and L_y are longitude and latitude, and R is the residual field not fitted by the linear model. The residual was interpolated using kriging as previously. Since $\phi = \phi(K)$, these calculations had to be done for each threshold value. Figure 27 shows the ϕ field that resulted for $K = 0^{\circ}\text{C}$ and $K = 5^{\circ}\text{C}$.

Recalculating the degree day maps with this correction resulted in a marked improvement in the maps. Figures 28 – 32 show the degree days before and after the correction. To enhance readability of the maps, locations with a degree day count of 1 or zero have been shaded gray. Clearly the gray zone expands with higher threshold values, but notice that for higher threshold values the extent of the gray color is far larger in the uncorrected maps. Figure 33 shows the difference between the corrected and uncorrected maps for chosen thresholds.

Three factors seem to affect the degree day count. Obviously, higher degree days are generally found at low altitude, and higher counts are obtained in southern Iceland. However, it is noticeable that in coastal valleys higher counts are obtained away from the coast, even though the altitude may be higher. This effect is clearly seen in the maps with a threshold value of 7°C and 10°C .

Maxima and minima of temperature

A further examination of summer time temperatures can be seen in Figure 34, which shows a map of the maximum mean temperature reached during the year, and also a map of the Julian day of maximum temperature. The figure shows that areas where the maximum temperature exceed 10°C are few, indeed 8°C is common in low lying areas. Maximum temperature is reached around Julian day 200, which is July 18th. This value is the most common one in the interior of the country and in the southern part. Along the coast, the date of maximum temperature is delayed by up to 3 weeks.

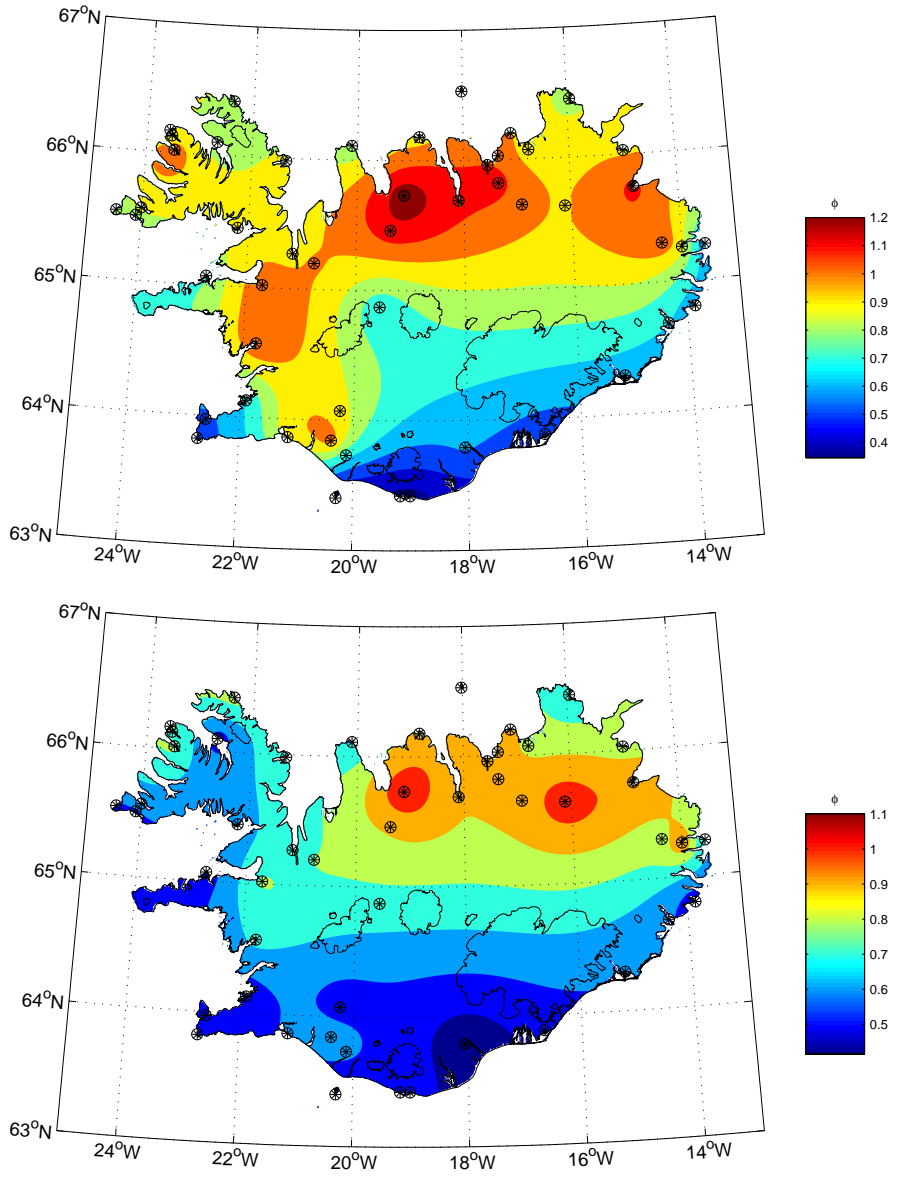


Figure 27: Examples of the correction factor ϕ for a threshold value of 0°C and of 5°C.

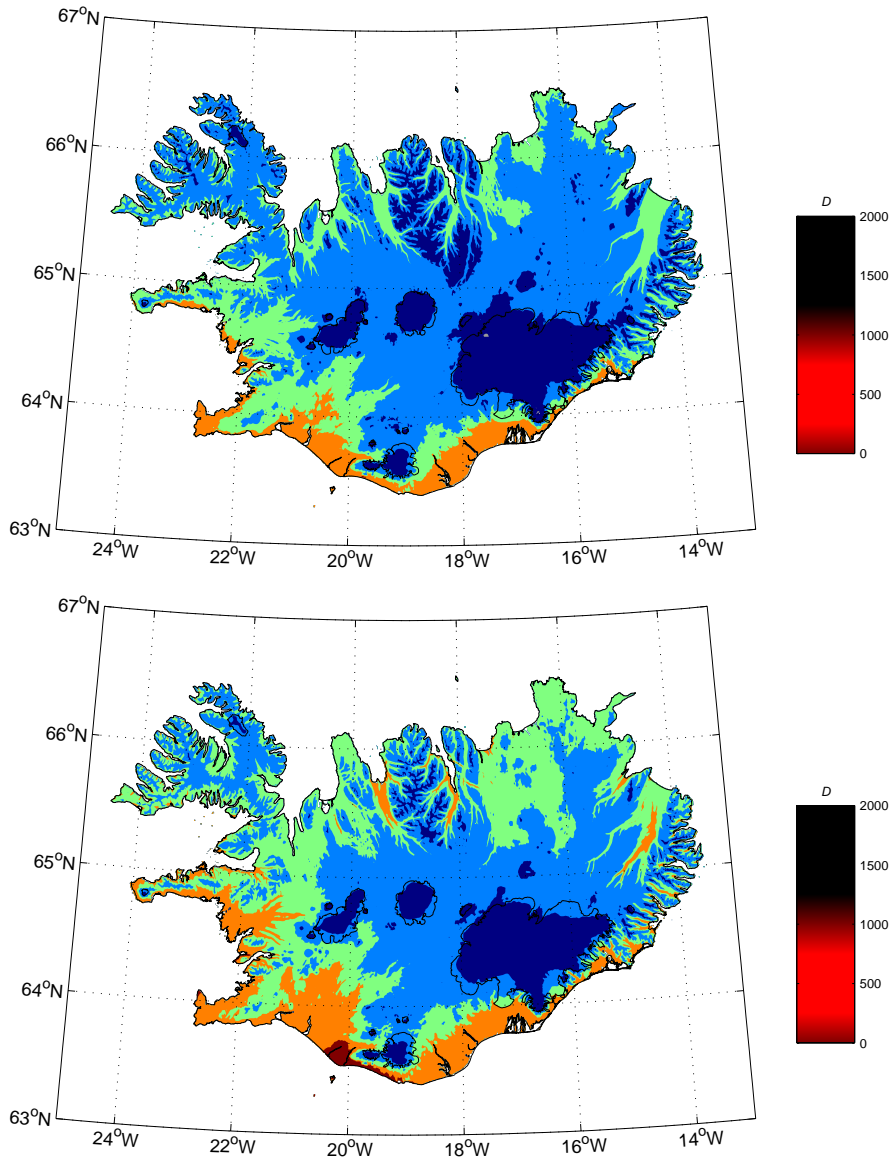


Figure 28: The degree day maps for a threshold value of $K = 0^\circ\text{C}$. The upper map shows the biased map, and the lower map shows the results with the bias corrected. Areas shaded with gray have a degree day count of 1 or less.

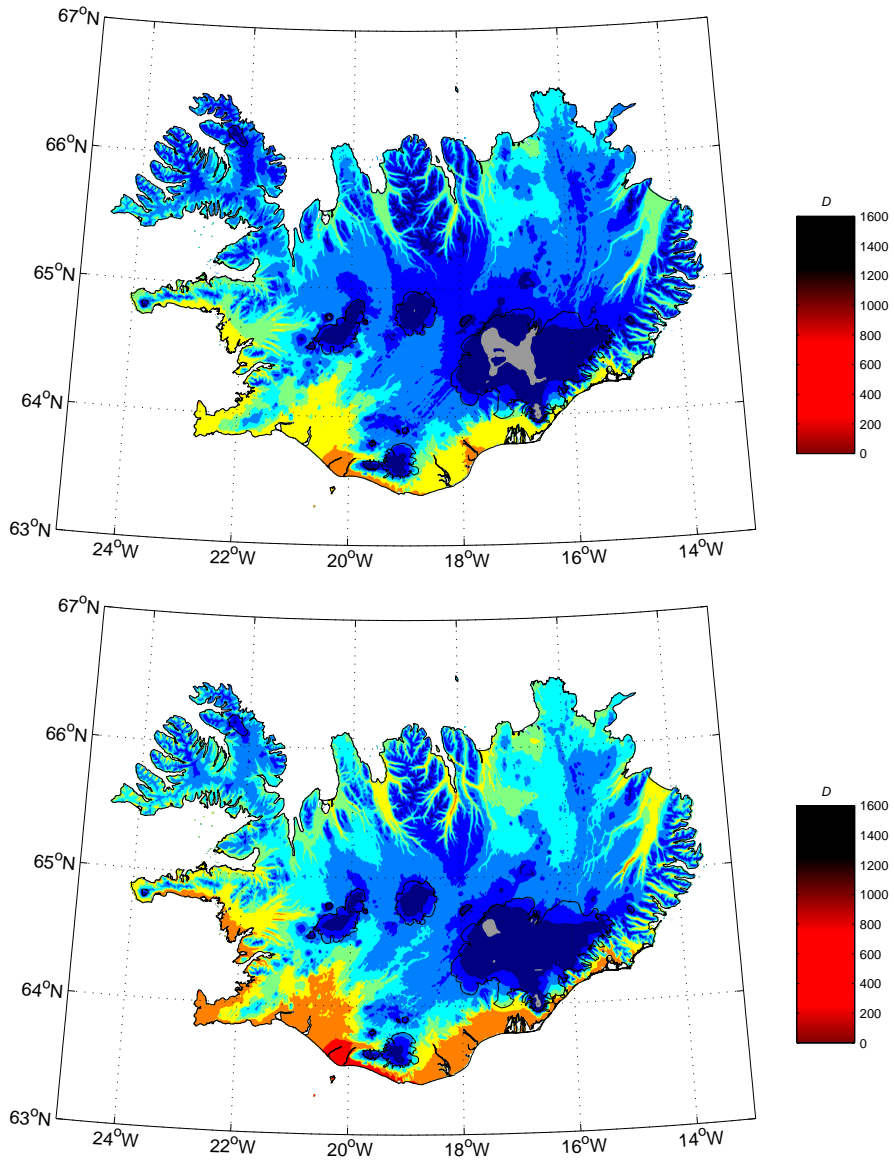


Figure 29: The degree day maps for a threshold value of $K = 2^\circ\text{C}$. The upper map shows the biased map, and the lower map shows the results with the bias corrected. Areas shaded with gray have a degree day count of 1 or less.

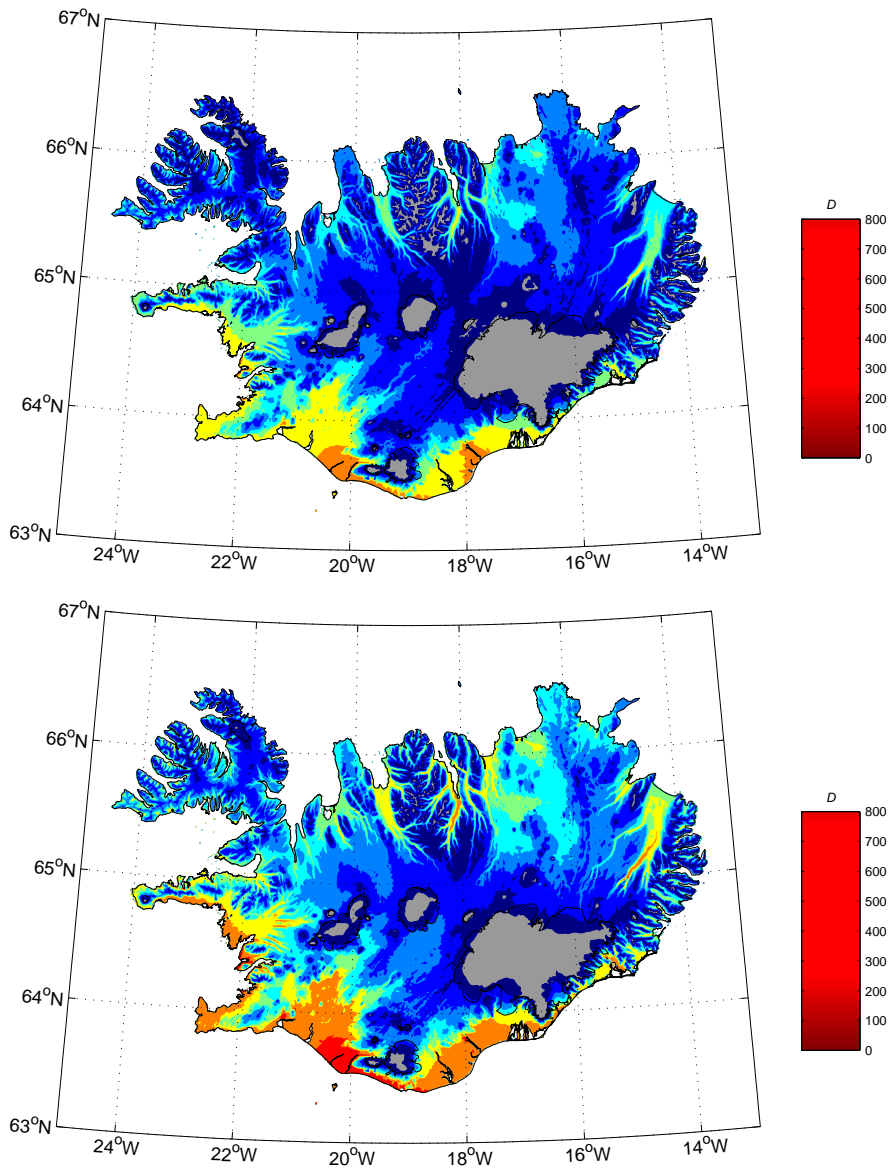


Figure 30: The degree day maps for a threshold value of $K = 5^\circ\text{C}$. The upper map shows the biased map, and the lower map shows the results with the bias corrected. Areas shaded with gray have a degree day count of 1 or less.

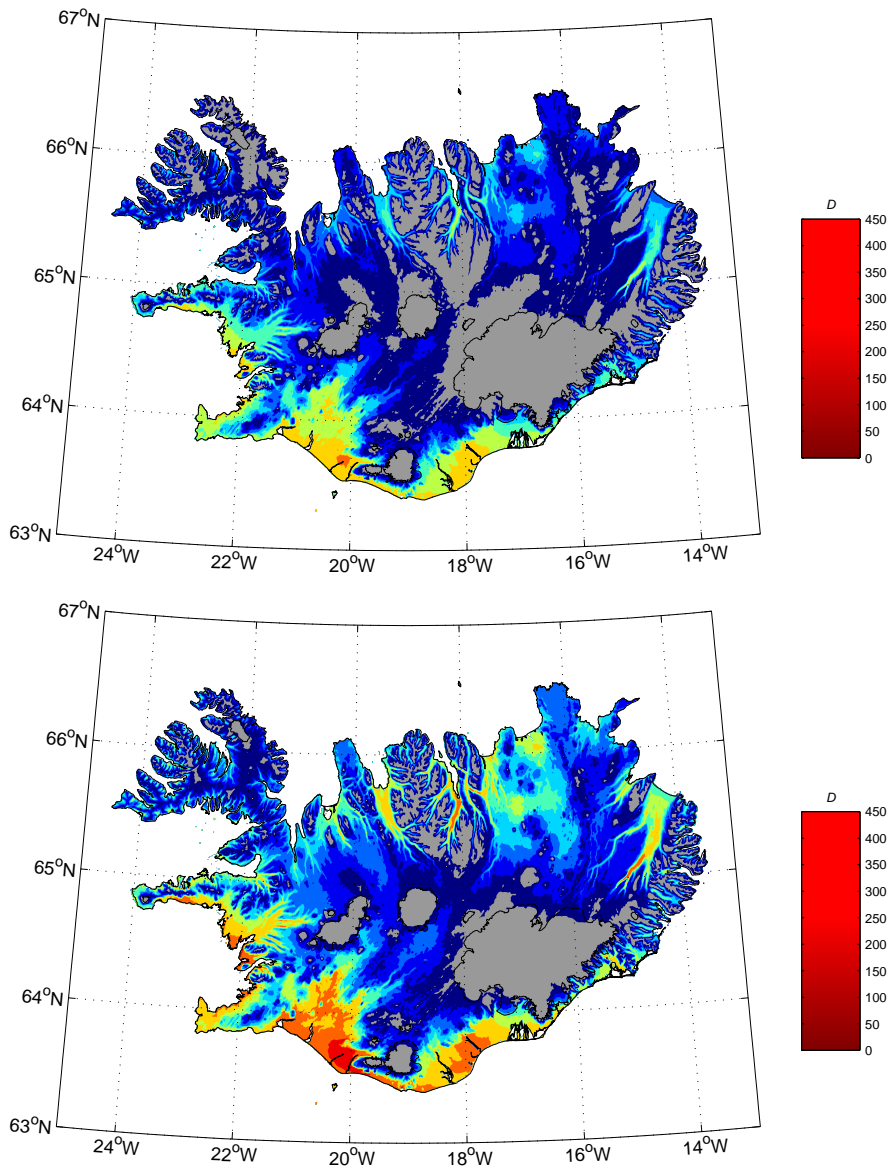


Figure 31: The degree day maps for a threshold value of $K = 7^\circ\text{C}$. The upper map shows the biased map, and the lower map shows the results with the bias corrected. Areas shaded with gray have a degree day count of 1 or less.

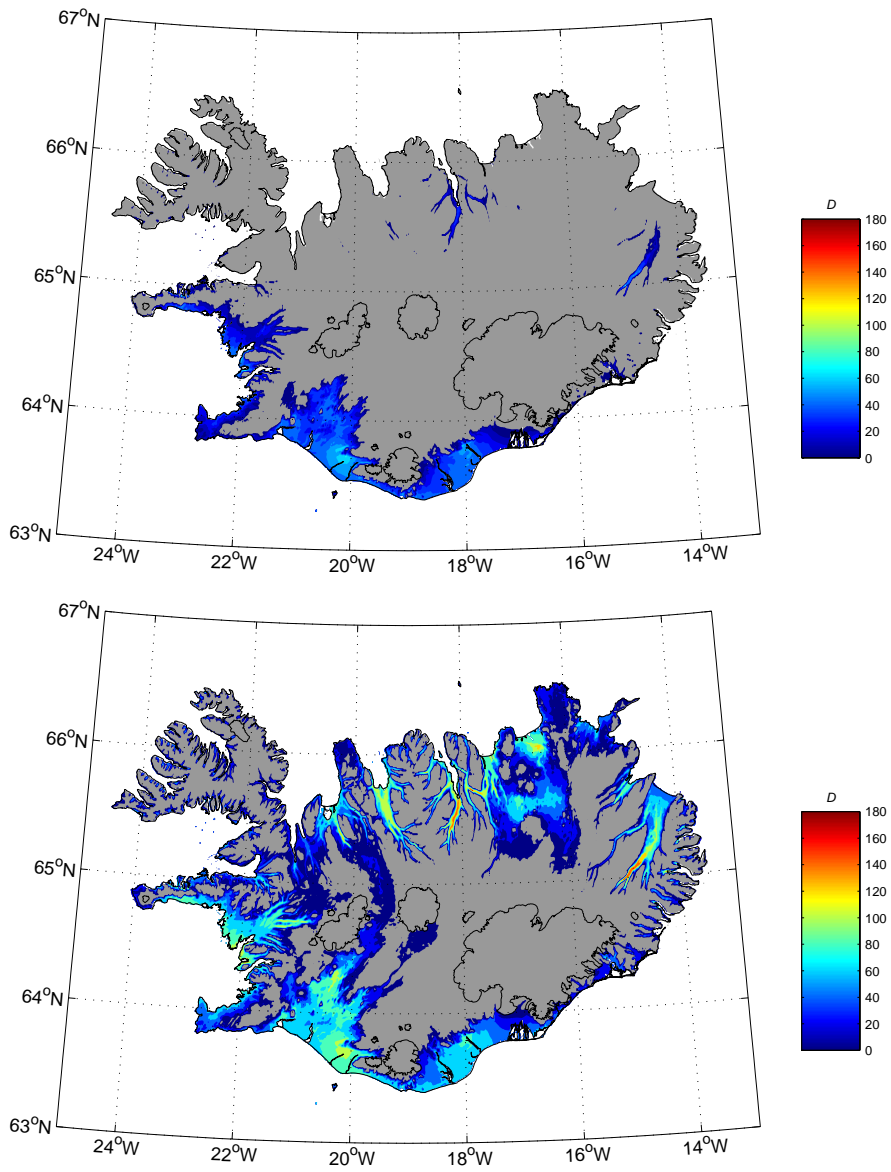


Figure 32: The degree day maps for a threshold value of $K = 10^\circ\text{C}$. The upper map shows the biased map, and the lower map shows the results with the bias corrected. Areas shaded with gray have a degree day count of 1 or less.

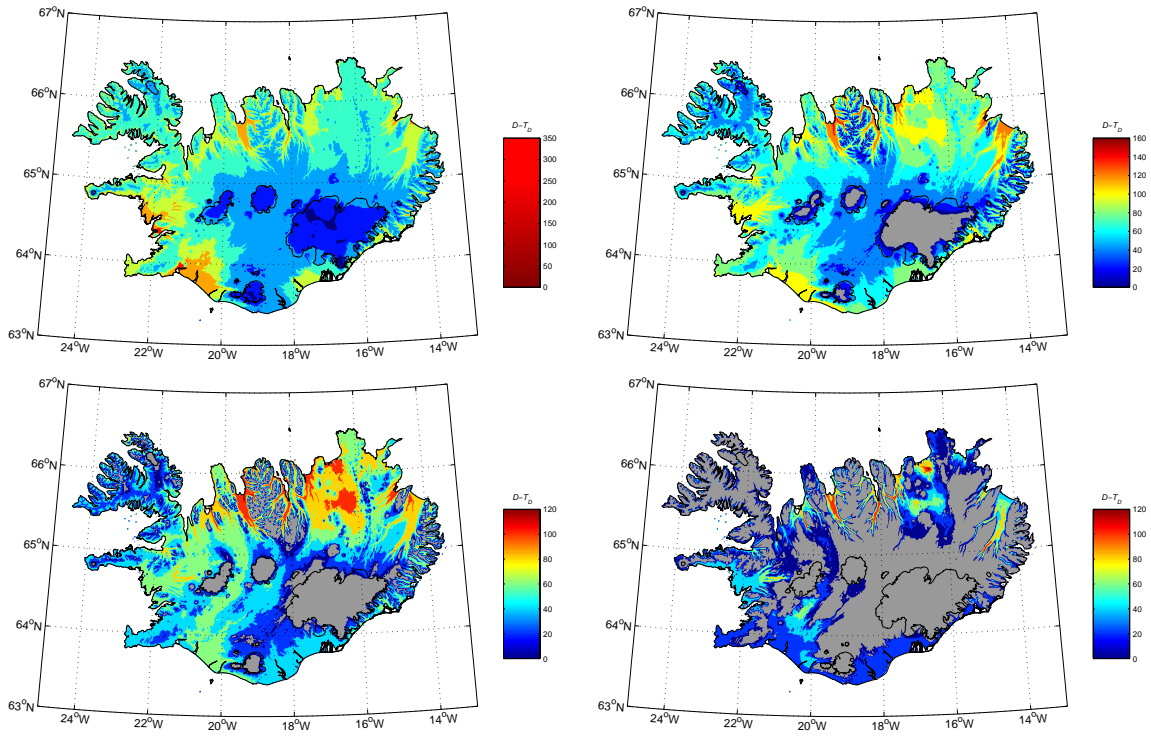


Figure 33: Differences between the corrected and the biased maps. The upper left panel shows the results for a threshold value of $K = 0^{\circ}C$, upper right panel shows the results for $K = 5^{\circ}C$, the lower left shows the results for $K = 7^{\circ}C$ and the lower right for $K = 10^{\circ}C$.

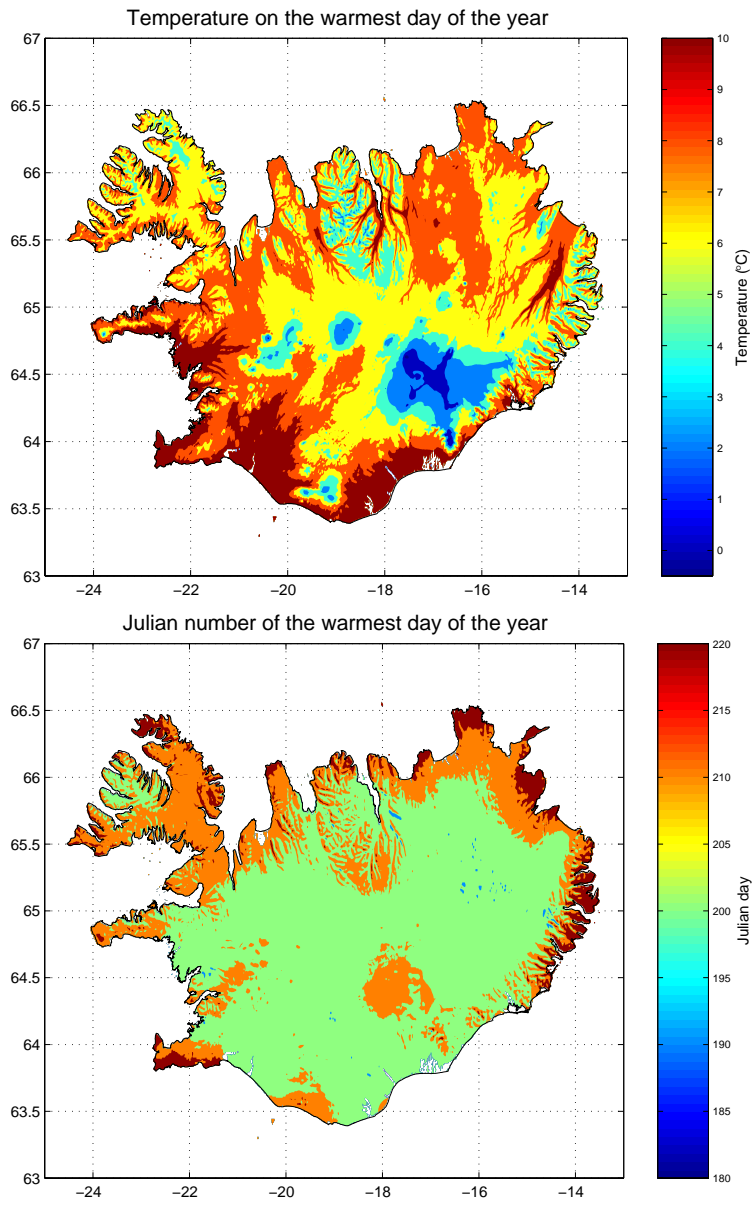


Figure 34: A map of maximum average temperature and the Julian day during which it occurred. Julian day 200 corresponds to July 18th.

The results of a similar calculation for the winter are shown in Figure 35, which shows the minimum temperature and the day on which it occurred. At the coast the minimum temperature ranges from 0 to -2°C , but from -2 to -6°C further inland. Minimum temperatures below -6°C occur at higher altitude. The map of Julian days shows that in some areas the minimum temperature is reached in December (Julian days around 350, located below zero on the colorscale). Throughout much of the country the minimum occurs in the middle of January, but in an area extending from Snæfellsnes peninsula on the west coast along peninsulas on the north coast to the fjords on the east coast, the temperature minimum occurs in March. This area corresponds to the area that is colder in March than in February (see Figure 21). Furthermore, the estimated date of minimum temperature also occurs during February or March over glaciers and a few high altitude areas.

Discussion

The maps presented herein, represent a first complete spatial analysis of the mean annual temperature cycle for the 1961 to 1990 period. The monthly mean temperature ranges from -5 to 7°C when averaged over the whole country, but when the average is limited to areas below 400 m the monthly mean temperatures range from -2 to 9°C . A cross-validation procedure reveals that the estimates are accurate within 1°C . Further analysis points to glaciers and high altitude areas as sites of possible systematic errors. For glaciers the method is expected to produce temperatures that are too high during the summer.

The analysis of daily mean temperatures revealed that along the south coast of Iceland, there are locations where the mean temperature never goes below freezing. During winter there is an area, roughly extending from the west coast along the north coast toward the east coast, where the winter temperatures have two minima, first in January and again in March.

The maps of degree-days produced using a method employed by the Nordklim group were also presented, but these maps are biased. The source of the bias was discussed in some detail. Following this a correction method was introduced and unbiased maps were presented. They show that while the degree day count is primarily a function of altitude, there is a north-south gradient, and coastal valleys tend to have higher counts inland, than at the coast.

An examination of the timing of the temperature maxima and minima revealed that during summer the maximum temperature is on average reached around July 20th throughout the interior of Iceland, but closer to the coast this date is postponed up to three weeks. During winter the location of the coldest day is more complex. In many locations days in late December or early January are the coldest, but there is a part of the country where the coldest days occur in March.

Acknowledgments

The author wishes to thank the many people who took part in this project. At different times, Sigríður Sif Gylfadóttir, Steen Henriksen and Einar Örn Ólason worked on this project and made integral contributions to it. Trausti Jónsson and Þórunn Pálsdóttir were instrumental in setting up the data base and their expertise was invaluable. The author would also like to thank Þór Jakobsson who read the manuscript and made several suggestions for improving it. Finally, members of the NORDKLIM group are

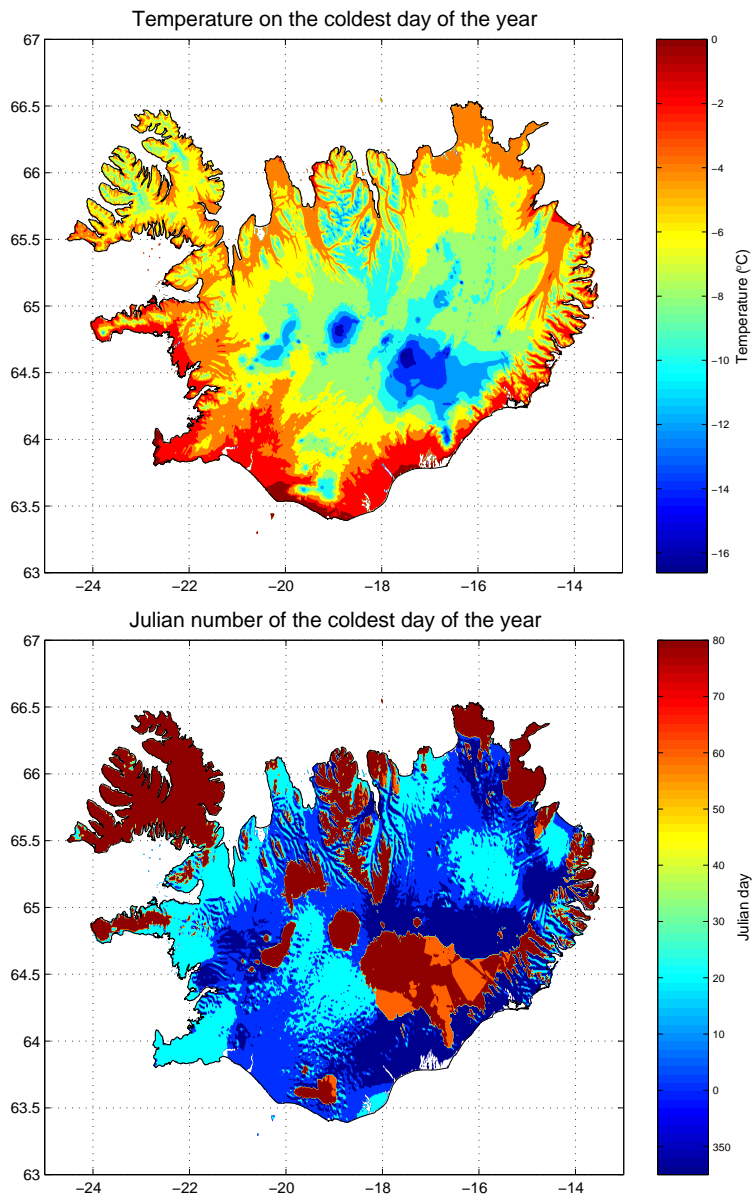


Figure 35: A map of minimum average temperature, and Julian day on which it occurred. Notice that in the lower panel, the colorscale is cyclic and December (335–365) is situated below January (1–31).

thanked for instigating work of this kind in the Nordic countries. Without their effort this project might never have taken off.

References

- H. Bjornsson. Eigenvectors of local topography in iceland. Technical Report 03007, Icelandic Meteorology Office, 2003.
- H. Bjornsson and T Jonsson. Climate and climatic variability at Lake Myvatn. *Aquatic Ecology*, 2003.
- H. Bjornsson and S. A. Venegas. A Manual for EOF and SVD Analyses of Climate Data. Technical Report 97-1, Center for Climate and Global Change Research, McGill University, 805 Sherbrooke West, Montreal, Canada, H3A 2K6, 1997.
- R. J. Braithwaite. Calculation of degree-days for glacier-climate research. *Z. Gletscherkd. Glacialgeol.*, 20:1–8, 1984.
- M. Einarsson. Climate of iceland. In H. E. Landsberg, editor, *World Survey of Climatology*, volume 15, chapter 7, pages 673–697. Elsevier, Amsterdam, 1984.
- J. Eythorsson and H. Sigtryggsson. The climate and weather of iceland. In E. Bertelsen, F. Gudmundsson, A. Ingolfsson, P.M. Jonasson, and S. L. Tuxen, editors, *The Zoology of Iceland*, volume 1, pages 1–62. Ejnar Munksgaard, Copenhagen, 1971.
- S. S. Gylfadottir. Spatial interpolation of icelandic monthly mean data. Technical Report 03006, Icelandic Meteorology Office, Reykjavik, Iceland, 2003.
- S. Henriksen. Report on the approximation of the annual cycle of temperature in iceland. Technical Report 03006, Icelandic Meteorology Office, Reykjavik, Iceland, 2003a.
- S. Henriksen. Applications of the tension spline method to 18 weather stations in iceland. Technical Report 03008, Icelandic Meteorology Office, Reykjavik, Iceland, 2003b.
- P. K. Kitanitis. *Introduction to Geostatistics: Applications in Hydrogeology*. Cambridge University Press, 1997.
- E. Ö. Ólason. Kvarðaleiðréttingar á Íslenskum gráðudagakortum (in icelandic). Technical Report 03035/UR24, Icelandic Meteorology Office, Reykjavik, Iceland, 2003.
- G. V. Middleton. *Data Analysis in the Earth Sciences Using Matlab*. Prentice Hall, New Jersey, 2000.
- O.E. Tveito, E. J. Førland, H. Alexandersson, A. Drebs, T. Jónsson, E. Tuomenvirta, and Laursen E. Nordic climate maps. Technical Report 06/01, DNMI, Oslo, Norway, 2001.
- G. Wotling, C. Bouvier, J. Danloux, and J. M. Fritch. Regionalization of extreme precipitation distribution using the principal components of the topographical environment. *Journal of Hydrology*, 233:86–101, 2000.